ADVANCED MATERIALS INTERFACES
Open Access
www.advmatinterfaces.de

Functionalized Antifouling Polymer Brushes for Biospecific Surfaces

Erik J. Postma, Luc Scheres, Sissi de Beer, Andriy R. Kuzmyn,* and Han Zuilhof**

Biosensors have become integrated into our lives. Current technology requires biosensors not only to have high sensitivity but also to have high specificity for one target, while repelling all other molecules and materials in the biological medium. These goals are met by surfaces that combine a biorecognition element and a high-quality antifouling layer. In this review, we largely focus on polymer brushes that are grafted from the surface, as these are known to exhibit excellent antifouling properties. We also discuss how to functionalize these with biorecognition elements. Based on the current research on antifouling brushes, we recommend using poly(2-hydroxypropylmethacrylamide) (HPMAA) and/or poly(carboxybetainemethacrylamide) (CBMAA) brushes, with a thickness between 20–30 nm. Furthermore, we note the importance of high polymer chain densities in such brushes and highlight that a proper comparison requires, among others, similar pre-treatments. These antifouling brushes are biospecific after receptors are integrated with efficient coupling strategies. Here the opportunities and limitations of frequently used approaches of antifouling polymer brushes within biosensors are highlighted. Also, with the resulting combination of high specificity and low (bio-)chemical noise levels, we envision an increase in the incorporation of novel polymer brushes for the development of stable biospecific sensors.

1. Introduction

Biosensors have become inseparable from our lives. The biosensor market size, estimated at 28.9 billion USD in 2023, is projected to reach 53.6 billion USD by 2031.[1,2] This market growth is caused by the increasing prevalence of chronic and lifestyle-related diseases and a growing elderly population worldwide,[2,3] leading to a growing interest in personalized medicine and health monitoring, which is driving near-patient and point-of-care testing. Therefore, point-of-care testing currently has the largest share in the global market, followed by laboratory-based applications, security, biodefense, and the food industry.[1,2] Examples of areas where sensors are applied include glucose monitoring for diabetes patients,[3,4] sensing of water quality for environmental reasons,[5] testing for COVID-19 and other infections,[6] and measurement of drug residues in food.[7] These applications have in common that they benefit from sensing devices that use biological recognition for diagnostic or therapeutic purposes.[8] Such a sensing device usually consists of a molecular recognition element (MRE) and a transducer that translates the MRE's response to an optical or electric signal that can be analyzed.[8,9] Transducers fall into three main categories based on their underlying mechanisms: optical detection, piezo vibrations, or electrochemical processes. Optical sensors use electromagnetic waves to detect biomarkers. Colormakers can translate the signal straightforwardly in point-of-care testing, for example, in pregnancy tests or COVID-19 test kits. Other types of optical biosensors include: optical fibers, ring resonators, interferometers, optical waveguides, photonic crystals, fluorescence/luminescence, and surface plasmons.[10–12] Surface plasmons are widely used with a broad range of research sensing applications.[10,13] For example, plasmons released by metal substrates, such as gold,

E. J. Postma, S. de Beer, A. R. Kuzmyn
Department of Molecules & Materials
MESA+ Institute
University of Twente
Enschede 7500AE, The Netherlands
E-mail: s.j.a.debeer@utwente.nl; a.r.kuzmyn@utwente.nl

The ORCID identification number(s) for the author(s) of this article can be found under https://doi.org/10.1002/admi.202400955

DOI: 10.1002/admi.202400955

L. Scheres
Surfix BV
Agro Business Park 2, Wageningen 6708 PW, The Netherlands
H. Zuilhof
Laboratory of Organic Chemistry
Wageningen University
Stippeneng 4, Wageningen 6708 WE, The Netherlands
E-mail: han.zulhof@wur.nl
H. Zuilhof
School of Pharmaceutical Sciences and Technology
Tianjin University
92 Weijin Road, Tianjin 300072, China
H. Zuilhof
College of Biological and Chemical Sciences
Jiaxing University
Jiaxing 314001, China

can induce Raman scattering in analytes near the surface. This surface-enhanced Raman scattering (SERS) affects the detection range and has been used to detect attomolar concentrations of analytes such as miRNA.[14–16] Furthermore, even single-molecule detection is nowadays possible with these optical techniques.[17] Besides SERS, Surface Plasma Resonance (SPR) is commonly used to detect biomarkers binding to surfaces.[18,19] SPR traces the changes in the refractive index of light when biomarkers bind to a surface.[20,21] This technique has detected analytes diluted to 10 aM and has detection limits down to 0.3 pg mm^{-2}.[22] Due to their high sensitivities, both SERS, SPR, and even a combination of these techniques, are currently used for sensing.[23,24]

Quartz crystal microbalances (QCM), which rely on piezo vibration, use a quartz crystal's resonance frequency to detect biomarker adsorption. Sensitivities of 10 and 5 MHz crystals can theoretically reach a detection limit of 44 and 177 pg mm^{-2} for a detectable change of one Hz, respectively. Even though the mass detection limit of these crystals is restrained by noise, QCM remains a well-integrated and sensitive research technique in laboratories.[25,26] Furthermore, in recent years QCM has been developed to sense thrombin,[27] food pathogens,[28] and SARS-CoV-2.[6] For the latter, the sensor reached a limit of detection (LOD) at $1.3 \cdot 10^4$ PFU·mL^{-1}.[6]

Electrochemical biosensors utilize current changes in an electrolyte solution to track the binding of target biomolecules to a sensor. For example, redox-active biomolecules (e.g., tyrosine or tryptophan) can selectively be absorbed into molecularly imprinted films.[29] In this case, a Faradaic current is measured within the redox window during cyclic voltammetry, chronoamperometry, or electrochemical impedance spectroscopy.[29–31] The current density during cyclic voltammetry is directly proportional to the analyte concentration in the solution.[29] However, since most biomolecules are not redox-active within the limits of most biosensors, an external redox reaction needs to facilitate the detection of the analyte. In these cases, the concentration of the analyte is indirectly measured from the current of the redox active species. This Faradaic reaction gets gradually prevented from occurring when the targeted biomolecules bind to the electrode and therefore the current density will correlate inversely with the analyte concentration.[29,30] A third method to sense biomolecules uses enzymes that produces redox-active species. These enzymes selectively attach to biomarkers that are immobilized on the surface. After rinsing off excess enzymes, the enzymatically generated redox-active molecules, result in Faradiac currents which correlate with the biomaker concentration.[32,33] Hydrogen peroxide is a common redox active species, which can be formed from a probe functionalized with lactate oxidase or horseradish peroxidase.[34–37] However, it's important to note that hydrogen peroxide is not always favorable due to its instability which can affect reliability. Many other redox-active species have been used such as NADP$^+$/NADPH,[38,39] methylene blue,[40,41] and ferrocene.[42,43] Other common electric biosensors are electric field transistors[44] and impedance-based sensors.[45,46] These electrochemical detection methods exhibit high sensitivities, with femtograms per milliliter range detection limits.[16]

While modern transducers offer extreme sensitivities, they encounter new challenges when applied to complex biological mixtures (such as blood, saliva, urine, and lymph).[47,48] Nonspecific interactions in these matrices lead to increased noise levels, loss of selectivity, drift, and challenges in regeneration and reuse.[49–52] In addition to hampering the selectivity, the durability also decreases when molecules irreversibly bind to the sensing area.[52] Specifically, cells, microorganisms, and proteins readily adsorb onto surfaces, forming biofilms.[53] Therefore, the development of accurate and reliable biosensors depends on the prevention of fouling on biosensors when exposed to complex matrices or in vivo testing.[49,52]

(Bio)fouling is the non-specific adsorption of biomolecules and organisms. This adsorption is primary caused by interaction between amino acids and the surface. These interactions consist of hydrogen bonds, ionic bonds, in some cases covalent bonds, and besides these bonds, hydrophobic- and hydrophilic interactions with a surface.[54,55] The complex structure of biomolecules allows multiple adsorption-related processes to occur that influence the adsorption rate simultaneously. For example, adsorbed biomolecules are replaced by others that have higher affinity for the substrate, which is called the Vroman effect.[56,57] Furthermore, surface crowding can induce protein rearrangements in the adsorbed layer, changing the number of binding sites and the affinity between the surface and the foulant during the adsorption process.[58]

Fouling is energetically least favorable at hydrophilic surfaces in aqueous solutions because of the energy barrier resulting from the competition with surface-bound water.[59,60] These desired solvating properties of surfaces are enhanced by net-neutral polar groups that are hydrogen bond acceptors.[49] Furthermore, steric repulsion also plays a role in influencing the antifouling properties of a surface.[61] However, biosensors typically lack the required properties to prevent fouling, as the surfaces consist of hydrophobic materials (e.g., graphene, modified metals, or polymers).[62] Fouling of sensors can be prevented by protecting the surface with hydrophilic polymers. In particular, covalently immobilizing polar polymers with one end to a functionalized surface enhances anti-fouling properties and sensor durability (**Figure 1**).[63–65]

These antifouling polymer brushes on the transducers allow for creating a more durable and selective sensor. By using optimal covalent attachment strategies,[62,66] the sensor not only gains long-term stability but also specific recognition for one single target from a large group of candidates (Figure 1C).[49] Polymer brushes can be divided into classes based on the chemical composition of their backbone. These classes include polysaccharides, poly(ethylene glycol) (PEG), polyacrylates, and polyacrylamides. The latter two are hydrophilic due to side chains containing zwitterionic, polar, or PEG moieties.[67] Polymer brushes have demonstrated wide-ranging applications—not only as antifouling coatings and advanced adhesive materials,[68] but also as antiviral surfaces[69] and antibacterial coatings.[70–71] They have been used in photosensitive systems for stimuli-responsive applications,[72] and in biointerfaces that support or regulate cell interactions.[73,74] In addition, polymer brushes have been employed to create lubricating surfaces with low friction and enhanced wear resistance.[75–77] More recently, they have even been explored for scent-distinguishing applications using chemically different polymer brush arrays.[78]

Furthermore, attaching recognition units such as specifically binding peptides (such as Arginylglycylaspartic acid (RGD)

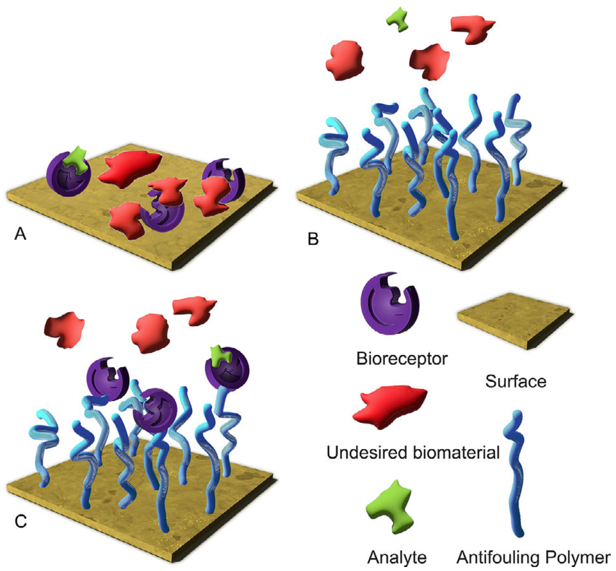

Figure 1. A) A surface with biorecognition elements (purple) is blocked by a complex mixture of fouled biomaterials (red), which hampers binding to the analytes of interest (green). B) With an antifouling polymer brush, the fouling of a wide variety of biomaterials on the surface can be strongly decreased. C) This increases the availability of biorecognition moieties and also reduces the (bio-)chemical noise, allowing the biorecognition element to exclusively bind to the analyte, which thereby can be detected by the transducer.

and antimicrobial peptides (AMPs)),[79] antibodies or derivatives thereof (llama antibodies,[80] immunoglobulins, etc.) to these antifouling polymer brushes ensure specific binding to a particular biomarker. This biospecific binding of targets depends, among others, on antibody orientation for which it is important that the paratope regions are directed outward. This is achieved by covalent binding (Section 3) or non-covalent binding strategies (such as immobilization by streptavidin).[70,71,81–83] The resulting combination of antifouling polymer brushes and these biospecific recognition units result in biosensors with optimal sensing conditions.

2. Antifouling Polymer Brushes

Antifouling polymer brushes offer a promising solution to the fouling problem by providing a surface that resists the adsorption of unwanted biological materials. These polymeric films are chains of polymers covalently attached to a substrate, forming a dense, brush-like layer. The design of these brushes allows them to create a hydration barrier at the sensor surface, reducing nonspecific interactions and preventing biofouling. This feature is particularly valuable for biosensors, where the accuracy and sensitivity of detection depend on the specificity of interactions between the sensor and the target analyte. **Table 1** shows antifouling polymer brushes with the reported specific amount of fouling in mass per surface area. We specifically focused on research from 2019 to 2024, in which brushes were grafted from the surface.

Polymer brushes are synthesized either by growing the polymer from initiators that are attached on the surface (i.e., "*grafting-from*"), or by covalently attaching polymers to the surface (i.e., "*grafting-to*"), or by a combination of the two (i.e., "*grafting-through*").[84–85] Limited success for antifouling layers has been obtained by grafting polymers to a surface, because "grafting-to" is prone to create lower grafting density polymer brush layers.[86–88] These relatively low-density brushes may not effectively shield the surface from adsorbing biomolecules.[86,89] One successful approach for "grafting-to" antifouling brushes has been obtained by attaching two ends of a polymer to a surface, creating a polymer loop.[90,91] Higher densities are obtained for these polymer loops, compared to linear chains that are grafted to the surface.[92] A second successful strategy grafts polymers to the surface with side chains that contain new initiator moieties.[86,93,94] By growing a bottle-brush polymers from these layers, a high-density layer is obtained with antifouling properties.[95] A third method obtained thick grafted-to polymer brushes on polydopamine by optimization of solvation conditions.[87,96]

With grafting-from, polymers are grown conventionally by either radical polymerization or ring-opening synthesis, as shown in Table 1. Free radical polymerization from a surface-bound radical initiator typically terminates before the desired thickness of >20 nm is obtained; therefore, reversible-deactivation radical polymerization (RDRP) techniques, with which such thicknesses are routinely feasible, have become the de facto standards in this field. RDRP controls polymer brush growth by adding a chain transfer agent (CTA) to reach an equilibrium between active and dormant chains. The two most common mechanisms for RDRP to grow polymer brushes with are atom transfer radical polymerization (ATRP) and reversible addition-fragmentation chain transfer (RAFT).[97,98] ATRP uses a transition metal, typically Cu(I), to abstract an organic halide (typically Cl or Br) from a dormant polymer chain and form a metal-halogen complex (**Figure 2**).[99,100] The resulting active organic radical proceeds with the polymerization until the metal redox reaction reverses or the polymerization is terminated. This equilibrium reaction ensures a controlled living polymerization, with typical polydispersities (M_w/M_n) <1.5.[99] ATRP is not oxygen tolerant, as Cu(I) readily oxidizes to Cu(II), which limits its application for scaling up.[101–102] However, new developments show how reductive species, such as ascorbic acid or glucose oxidase, can regenerate activators by electron transfer (ARGET).[103–107] Particular, ARGET-ATRP has become a method that allows non-experts to easily graft polymer brushes.[106,108,109] Besides ATRP, which uses Cu(I), single-electron transfer living radical polymerization (SET-LRP) utilizes the decomposition of Cu(I) into Cu(0) and Cu(II). In these polymerizations, the highly reactive Cu(0) exclusively activates the polymerization.[110]

Ring-opening polymerizations involve cyclic monomers, such as lactones, opening while attaching to a polymer on the surface. This equilibrium reaction is typically driven by the release of ring strain, which facilitates the formation of linear polymer chains. Degrafting of these polymers is often feasible, because of the heterogenous atoms in the backbone of the polymer.[111–113]

In contrast to ATRP, RAFT uses no (heavy) metal catalysts, but organic ones which deactivate active chains by covalent binding of the CTA.[114,115] Upon binding, the CTA can fragment and activate a second radical. Typically, the CTA contains a thiocarbonylthio group with a "Z-group" (see Figure 2) that is chosen to stabilize the intermediates to different degrees by

Table 1. Antifouling polymer brushes, initiated from surfaces, combined from recent studies.

Polymer brush	Method	Dry thickness [nm]	Fouling [pg mm^{-2}]	Refs.
Homopolymers (non-charged)				
HEMA 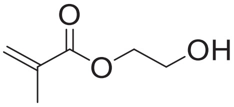	ATRP	12	<100(BP)	[132]
		25	1070(BP)	[133]
HEA 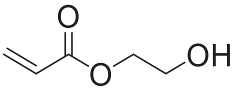	ATRP	19	<100(BP)	[132]
MEA 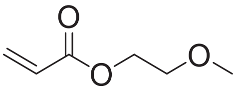	ATRP	11	≈200(BP)	[132]
HPMA 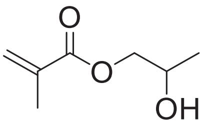	ATRP	30	<0.3(Fbg, IgG, Lyz, HSA) 410(BP)	[22]
HPMAA 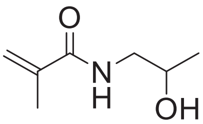	ATRP	17	<0.3(Fbg, IgG, Lyz, HSA, BP)	[22]
		30	<1(BP)	[74]
		48	≈100(BP)	[134]
	SET-LRP	30	<LOD(Lyz, HSA) 10(BP)	[135]
		50	<LOD(Lyz, HSA) 30(BP)	[136]
	RAFT	14	≈30(HSA, Fbg, BP)	[89]
	PET-RAFT	37	10(HS)	[118]
HOEGA 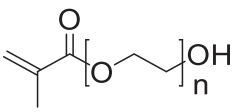	ATRP	1	1096(BSA)	[105]
		4	3304(BP)	[105]
		6	232(BSA)	[105]
		13	≈0(BSA) ≈50(Fibronectin) ≈100(FBS)	[137]
	ATRP-GOx	6	166(BSA)	[105]
		6	2358(BP)	[105]
		9	−215(BSA)	[105]
MeOEGA 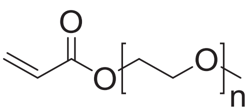	PET-RAFT	39	37.9(Lyz)	[138]

(*Continued*)

Table 1. (Continued)

Polymer brush	Method	Dry thickness [nm]	Fouling [pg mm^{-2}]	Refs.
		70	60.9(Lyz)	[138]
		99	44.2(Lyz)	[138]
MeOEGMA	ATRP	11	<100(BP)	[132]
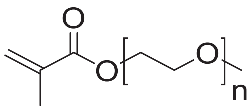				
		25	44(BP)	[139]
		30	<0.3(Fbg, IgG, Lyz, HSA) 230(BP)	[22]
	PET-RAFT	27	126(HS)	[118]
MSEA	PET-RAFT	23	1440(Lyz)	[138]
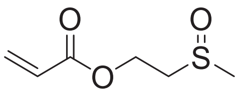				
		70	326(Lyz)	[138]
		98	34.7(Lyz)	[138]
NMEP	ATRP	20	120(BSA) 630(Fbg) ≈1300(Serum)	[140]
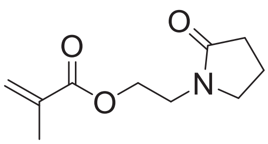				
IPOx	RDRP	15	<LOD(BSA, Fbg, FBS), ≈200(BP)	[141]
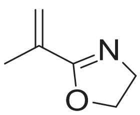				
NVP	UV- LRP	9	318(BSA) 2431(Fbg) 1184(Lyz)	[142]
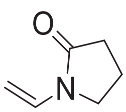				
DLA	SET-LRP	30	120(HSA) 20(Lyz) 960(BP)	[135]
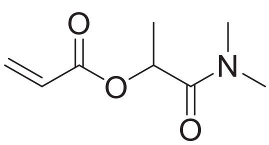				
		140	<LOD(HSA) 20(Lyz) 50(BP)	[135]
Oligo(2-methyl-2-oxaoline)methacrylate	ATRP	12	≈50(BSA) ≈75(Fibronectin) ≈500(FBS)	[137]
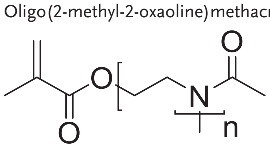				
Oligo(2-ethyl-2-oxaoline)methacrylate	ATRP	12	≈200(BSA), ≈150(Fibronectin), ≈800(FBS)	[137]
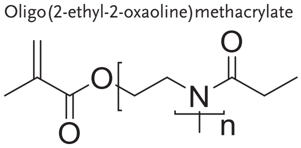				

(*Continued*)

Table 1. (Continued)

Polymer brush	Method	Dry thickness [nm]	Fouling [pg mm^{-2}]	Refs.
		21	≈50(BSA), ≈0(Fibronectin), ≈75(FBS)	[137]
Para-OEGAB 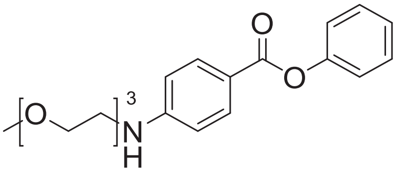	CGC	20	250(BSA)	[143]
Meta-OEGAB 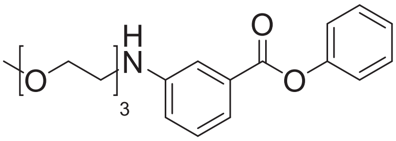	CGC	20	<LOD(BSA)	[143]
EtPPn 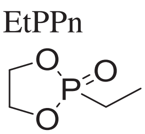	ROP	25	20(HSA) 170(HS) 100(Fbg)	[112]
Homopolymers (zwitterionic)				
CBAA 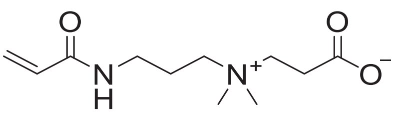	ATRP	12	<1(BP)	[74]
		18	<0.3(Fbg, IgG, Lyz, HSA, BP)	[22]
		20	9(BP)	[144]
		39	≈50(BP)	[134]
		N/A	500(BP)	[145]
	ARGET-ATRP	25	24(Serum)	[109]
CBMAA 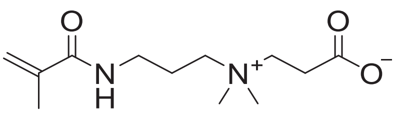	ATRP	13	<1(BP)	[74]
		14-21	≈300(BP)	[146]
		39	≈100(BP)	[134]
	PET-RAFT	36	14(HS)	[118]
SBMA 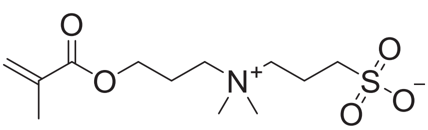	ATRP	105	≈1100(BSA)	[147]
SBMAA 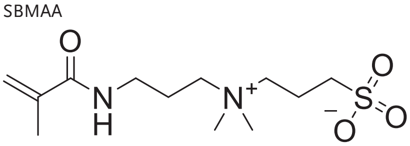	ATRP	17	≈700(BP)	[134]

(*Continued*)

Table 1. (Continued)

Polymer brush	Method	Dry thickness [nm]	Fouling [pg mm^{-2}]	Refs.
MPAO 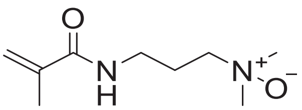	SI-ATRP	N/A	619.5(BSA)	[148]
NICPS 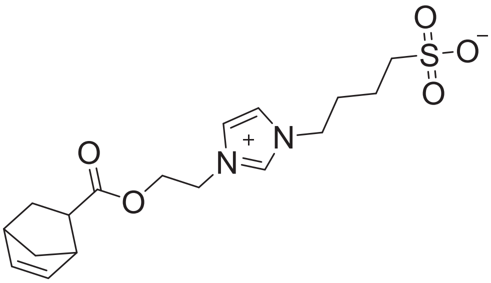	ROMP	N/A	156.3(BSA)	[149]
Co-polymers				
Poly(HPMAA)-*block*-poly(CBMAA)	PET-RAFT	40	40(HS)	[118]
Poly(HPMAA-*co*-CBMAA)	PET-RAFT	53	53(HS)	[118]
	ATRP	31-36	<1(BP)	[74]
		N/A	≈100(BP)	[145]
	SET-LRP	30-40	230(HSA)	[150]
		44	117(BP)	[151]
Poly(HPMAA)-*block*-poly(HPMAA-*co*-C12+[1)])	SET-LRP	50	20(Lyz) <LOD(HAS) 40(BP)	[136]
Poly(HPMAA-*co*-CBMAA-*co*-SBMAA)	ATRP	50	109(BP)	[152]
Poly(OEGMA)-*block*-poly(3-azidoHPMA)	ATRP	34	≈500(BP) ≈250(Luria-Bertani medium)	[153]
Poly(HOEGMA-*co*-Sodium 4-vinyl-benzenesulfonate)	RDRP	N/A	≈1050(Fbg)	[154]
Poly(HEMA)-*graft*-poly(NVP)	UV- LRP	10	34(BSA) 637(Fbg) 541(Lyz)	[142]
Poly(SBMA)-*block*-poly(MAA)[2)]	ATRP	172	800(BSA)	[147]

"≈" indicates an estimation of the fouling from a graph. Used abbreviations: Atom transfer radical polymerization (ATRP), Single-electron transfer-living radical polymerization (SET-LRP), Reversible addition fragmentation chain transfer (RAFT), Photoinduced electron transfer reversible addition fragmentation chain transfer (PET-RAFT), Atom transfer radical polymerization with glucose oxidase (ATRP-GOx), Activators regenerated by electron transfer (ARGET), Reversible-deactivation radical polymerization (RDRP), Ultraviolet initiated living radical polymerization (UV-LRP), Chain-growth condensation (CGC), Ring opening metathesis polymerization (ROMP), Ring opening polymerization (ROP), Limit of detection (LOD), Blood plasma (BP), Fibrinogen (Fbg), Immunoglobulin G (IgG), Lysozyme (Lyz), Human serum albumin (HSA), Human Serum (HS), Bovine serum albumin (BSA), Fetal bovine serum (FBS). Monomers are also abbreviated: Acrylate (A), Methacrylate (MA), Acrylamide (AA), Methacrylamide (MAA). [1)] *N*-(3-methacrylamidopropyl)-*N*,*N*-dimethyldodecan-1-aminiumiodide; [2)] Poly(Methacrylic acid.

π-delocalization.[98] For grafting-from polymer brushes this thiocarbonylthio moiety is preferably attached to the surface with its sulfur, to ensure that only ≈50% of the polymers will be formed in solution and 50% of the polymers will reside on the surface.[116,117] Conventional RAFT is, like conventional ATRP, not oxygen tolerant, which limits applications.[101,117] However, photoinduced electron transfer-RAFT (PET-RAFT), which uses eosin Y as a photocatalyst, is oxygen tolerant in combination with triethanolamine.[69,73,114,118–124] Both ATRP and RAFT require the initiator to be attached to the surface for a "grafting-from" polymer brush. ATRP is initiated by a halogen as initiator, which is often a tertiary bromine which stabilizes the formed carbon radical. Typical initiators are α-bromoisobutyryl bromide (BiB) derivates, that are anchored to surfaces such as metals, graphene, and silica.[64,125,126] RAFT requires thiocarbonylthio derivates to be attached to anchors on a surface, which is readily performed by active ester coupling.[114,118,127] For gold, alkane thiol-based anchors are commonly used because high-density monolayers are obtained by self-assembly.[28,66,128] Hydroxyl-terminated surfaces, such as silica, commonly use anchors that hydrolyze on the surface, such as (3-Aminopropyl)triethoxysilane (APTES).[66,127] Furthermore, polydopamine surfaces have been readily functionalized with BiB initiators, via esterification of hydroxyl and amine groups.[87,129,130] Finally, a reversible, supramolecular attachment that may work on a wide variety of surfaces has recently been demonstrated using cyclodextrin-adamantane-based host-guest chemistry.[131] The monomers that were recently used to form antifouling brushes on these layers are listed below in Table 1.

The following paragraphs describe the design parameters which affect antifouling properties of polymer brush surfaces. Table 1 already indicates a wide range of monomers and resulting fouling levels, which find their origin in chemical structure, the

ADVANCED MATERIALS INTERFACES
Open Access
www.advmatinterfaces.de

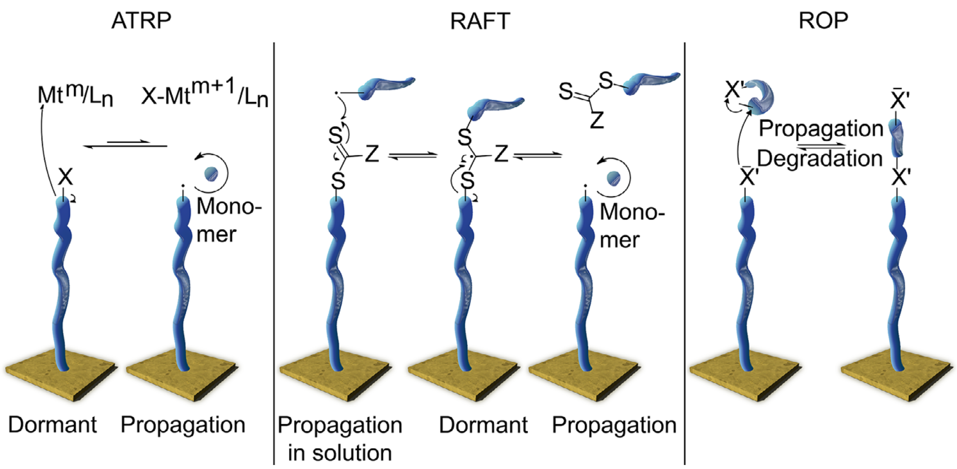

Figure 2. Reaction mechanisms of ATRP, RAFT, and ROP during the propagation of the brushes. X represents a halogen, like Br or Cl, Mt is a transition metal, L_n is a ligand, X' is a nucleophile such as oxygen, phosphor, or nitrogen.

conformation of chains, and external conditions. **Figure 3** provides a full overview of these parameters, with indicated section numbers referring to the location of discussion.

2.1. Monomers

Nowadays, a wide variety of monomers are available to prevent the irreversible binding of proteins, plasma, and other biomolecules from complex matrices. The most commonly used polymer brushes are acrylates and acrylamides with a wide variety of polar non-charged groups (e.g., HP(MA)A, HE(MA)A, MSEA, and ethylene glycol derivatives) or with zwitterionic moieties, (e.g., SB(MA)A, and carboxy betaines). Slight differences in the fouling behavior of these sidechains, particularly when exposed to complex media, can significantly impact the suitability of a particular polymer brush for use in sensing applications. These subtle variations ultimately determine which polymer brush is most effective in a given context, because these values contribute to the lower detection limits of sensor biomarkers. Generally, we noted that HPMAA is often chosen as a monomer, and in copolymers often combined with zwitterions like CBMAA. This is not surprising, since extremely low fouling (<0.3 pg mm^{-2}), below the detection limits of SPR (let alone QCM), has been reported for HPMAA.[22,74,135,136]

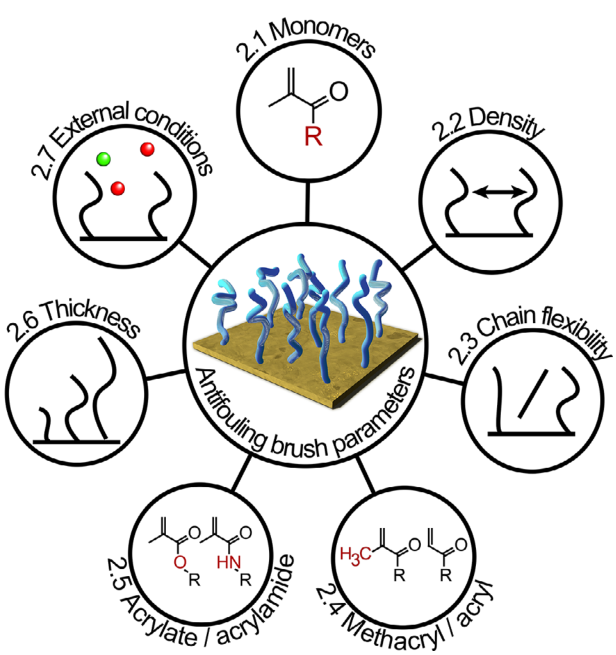

Figure 3. Overview of the chapters in Section 2, which discuss the parameters that influence the antifouling properties of polymer brush surfaces.

2.1.1. Monomer Selection Based on Hydration Layer

The reason why certain monomers outperform others, is based on several properties, such as hydrophilicity, length of side chain, and cohesive interaction between different polymers. The latter two strongly influence steric hindrance. Early research already showed that fouling increases with more apolar carbons in the side chain, for example, poly(2-hydroxyethyl methacrylate) has less fouling in serum and blood plasma compared to poly(3-hydroxypropyl methacrylate).[155,156] More recently, Andel et al. showed that for zwitterionic sulfobetaines the amount of carbons between the charged amine and sulfur matter for fouling. Specifically, they measured with fluorescence 3 times less fouling in serum on side chains with 2 carbons between the charges, compared to a distance of 3 carbons.[157] Similar results were found with SPR for carboxy betaines, which show excellent low fouling of serum on monomers with 1 and 2 carbons between the charged groups, though more than 10 times more fouling for 3 carbons.[158] Sarker et al. explained this effect by a decrease in dipole moment for less charge separation in zwitterionic materials, which in turn improves hydrogen bonding with water.[159]

2.1.2. Monomer Selection Based on Novelty

Currently, new monomers are still being developed. Singh et al. synthesized polyoxazolines and showed how to graft new polymers from these moieties.[141] This poly(2-isopropenyl-2-oxazoline) itself showed no detectable fouling of BSA, FBS, and Fbg on SPR. Pérez et al. researched biodegradable and biobased polymer brushes with phosphorester backbones by ROP.[112] Their research found that poly(2-ethyl-2-oxo-1,3,2-dioxaphospholane) prevented fouling of HSA (20 pg mm^{-2}), diluted serum (170 pg mm^{-2}), and Fbg (100 pg mm^{-2}). And in 2019, a new class of antifouling trimethyl N-oxide derived zwitterionic polymers was published by Li et al.[160] These new monomers with new properties increase the applications of brushes in biosensors.

2.2. Density and Steric Hinderance

Hydration is a critical factor influencing antifouling performance, as water molecules create a structured hydration layer that resists protein adhesion.[161] The length of polymer chains grafted onto a surface influences their ability to form an effective steric barrier against fouling. Longer polymer chains provide greater configurational entropy and steric hindrance, reducing the probability of biomolecule adsorption.[162] Brush density refers to the number of polymer chains per unit area on a surface. High brush densities enhance steric repulsion and hydration. While film hydration, chain length, and polymer brush density each contribute to antifouling efficacy, their interplay is complex and context-dependent. Hydration provides a crucial repulsive force, but it must be complemented by optimal polymer chain length and density to maximize steric effects.

Several studies from the last few years suggest that steric hindrance affects fouling. Steric hindrance originates from the structure and density of the brush.[163] Wang et al. compared fouling of linear polymer brushes with bottle-brushes of poly(*N*-vinylpyrrolidone).[142] Bottle brushes reduced the amount of fouling compared to linear brushes for BSA (89% fouling reduction), Fbg (74% reduction), and Lyz (54% reduction). The brushes had similar thicknesses and similar densities of initiator at the surface, causing in the bulk a higher density of polymer for the bottlebrush. These density differences are key to increase steric hinderance and limit fouling.[89,132] Yoshikawa et al. researched this effect on functionalized silica nanoparticles.[132] They synthesized brushes with different densities by functionalization of the surface with ATRP initiator and a non-reactive group in different ratios. The resulting lowered polymer densities caused an increase in human plasma fouling for all brushes (poly(PEGMA), poly(MEA), poly(HEMA), and poly(HEA)).

2.3. Chain Flexibility

Besides density, the flexibility of the polymer (side)chains was found to be important to improve fouling resistance. For example, Reese et al. found differences in fouling on *meta* and *para*-substituted aromatic polyamides with oligoethylene glycol side chains.[143] *Meta*-substituted arylamides showed no BSA fouling with QCM, whereas *para*-substituted arylamides had an average BSA fouling of 250 pg mm^{-2}. Compared to their *para* analogs, AFM force-distance curves also showed strong repulsive forces for *meta*-substituted polymers. These differences were explained by the formation of densely packed OEG chains, which can form in the more flexible *meta*-substituted polymer chains.

2.4. Methacryl or Acryl

In acrylic-based brushes, the properties of the backbone can be altered by a methyl group, which is obtained from methacrylates or methacrylamides. Methacrylic polymers with short sidechains are known to have higher glass transition temperatures than acrylic ones, however, predicting the flexibility of these chains remains complex.[164] Studies do indicate that less fouling is often obtained from methylacrylics.[165–167] A difference of 20 pg mm^{-2} of serum and plasma fouling has been measured in favor of HEMA over HEA polymer brushes.[166] Furthermore, Koschitzki et al. measured with fluorescence an improved fouling resistance of CBMA compared to CBA in a copolymer.[167] These findings are counterintuitive from a pure hydration layer perspective since methacrylates are known to have less hydration than acrylates.[168] However, the complex interplay between hydration layer and other physical properties of the brush favors in this case methylacrylates, for their high glass transition temperature which is typically above room temperature. The glass-like behavior causes the polymers to conform less to the biomolecules and therefore, possible interactions between matrix and surface remain limited.[165]

2.5. Acrylate or Acrylamide

Acrylamides tend to have superior antifouling behavior compared to their acrylates.[166] When comparing SBMA and SBMAA, or HEA and HEAA, the acrylamides outperform the acrylates in fouling resistance.[169] Zhao et al. measured the equilibrium water content in hydrogels of these polymers and showed that acrylamides enhance surface hydration at all tested crosslink densities.[169] A possible explanation might be that amides form a stronger surface hydration because they act both as hydrogen-bond donors and acceptors toward water.[166]

2.6. Thickness

Studies from Table 1 use different thicknesses of antifouling layers. An extensive correlation between fouling and thickness of poly(HEMA) and poly(HPMA) was performed by Zhao et al. for Fbg, BSA, Lyz, serum, and plasma.[155] They showed that these layers become anti-fouling around 20–30 nm, comparable with thicknesses often used in literature (see Table 1).[112,137,138,155] We attribute this to two factors: First, with such thicknesses any substrate surface-specific features are fully overruled by the characteristics of the polymer brush. Secondly, with a high enough surface density of the initiator, the resulting density of the attached polymer chains is high enough to nearly completely "overgrow" small surface defects, due to either nm-sized substrate defects or some inhomogeneity in the initiator density. This effect, of course, continues to improve surfaces if the polymer brush gets even thicker. However, with thicknesses of more than 30 nm the antifouling layer often does not improve, and in some cases, even slightly worsens.[170,171] For example, Zhoa et al. found that for brushes of poly(3-hydroxypropyl methacrylate) minimum, Fbg fouling was reached ≈29 nm (<3 pg mm^{-2}), however, at 35 nm and 39 nm brush thicknesses the fouling increased to 53 and 56 pg mm^{-2} respectively.[170] We hypothesize that this fouling increase at thicker brushes is linked to several factors, such as an increase in the molecular weight of polymer chains, a decrease in density in the upper part of the brush due to chain termination, and, consequently, a higher polymer dispersity. Previously, a thin poly(HPMA) brush with a thickness of 13.5 nm was reported to have a molecular weight of 49000 g·fmol^{-1} and a grafting density of 0.18 chains per nm^2,[89] and a poly(MeOEGMA) brush with a thickness of 10 nm had a molecular weight of ≈100 000 g mol^{-1} with a grafting density of 0.07 chains per nm^2.[121] Therefore, polymer brushes with thicknesses exceeding 30 nm are expected to exhibit significantly higher molecular weights. The longer chains may increase the tension at the anchor points and, therefore, cause degrafting.[66] To the degree that this is an issue, it can be improved with better anchoring chemistries, such as introducing poly(GMA) macroinitiators.[111] Moreover, as the polymerization process continues to achieve greater thicknesses, a reduction in polymerization control becomes inevitable, leading to chain termination. This, in turn, reduces the polymer density in the upper part of the brush and increases the polydispersity, which may also contribute to antifouling properties. Thus we see a typical optimum brush thickness reached when the "overgrowing effect" has been more or less completely obtained, but the detrimental heterogeneity and increased tension are still limited. Therefore, we recommend using brushes with 20–30 nm dry thicknesses for optimal sensitivity in sensing techniques and antifouling studies.

2.7. External Conditions

The fouling of polymer brushes in different environments can vary, though often not significantly. For example, Víšová et al. showed that fouling depends on the preconditioning of the layer and the ions in the buffer.[134] Their research compared the fouling of undiluted blood plasma with and without drying steps on CBAA, CBMAA, SBMAA, and HPMAA polymer brushes. For all four polymer brushes, the fouling decreased after rehydration, in some cases by more than 50%. It was supposed that higher levels of hydration, which occur upon rewetting the polymer brush, create an improved water shell over the surface.[155,172] In addition to drying, the interaction of ions with the brush and proteins changes the hydration layer and structure by salting in (kosmotropic) or salting out (chaotropic), which influences fouling.[134,173] These changes in fouling can impact the fouling of complex mixtures in particular. Blood plasma varies in composition and ion concentration, and therefore, fouling tests depend on the plasma donor.[48,133,139] Riedlová et al, studied the fouling of 50 donors on MeOEGMA brushes and noted fouling ranging from 1.2–2290 pg mm^{-2} depending on the donor.[139]

The recent research on polymer brushes has led to a deeper understanding of how brush properties affect fouling. Overall, the "grafted-from" polymer brushes based on CBMAA and HPMAA monomers and their synthesized copolymers showed the most effective antifouling against numerous biological fluids. The optimal thickness of the polymer brush to show effective antifouling is recommended to be in the range 20 to 30 nm. Furthermore, high densities and rehydration of the brush lead to improved antifouling properties.

3. Biofunctionalization of Antifouling Polymer Brushes

Combining antifouling polymer brushes with biorecognition or biointeractive elements, like an aptamer, peptide, or antibody, can create biospecific surfaces.[49] It is crucial to preserve the antifouling properties of polymer brushes during this process, as the biospecific surfaces should have only specific interactions with a particular analyte. The immobilization of a biointeractive element on the polymer brush can be conducted using different chemistries:[174,175] nucleophilic exchange,[176,177] thiol-ene and thiol-yne additions,[178] alkyne-azide cycloadditions,[179–182] thiol-maleimide additions,[183] Diels–Alder reactions,[184] and active ester couplings (**Figure 4**).[185–186] We further anticipate that future research will incorporate biomolecules into brushes using a wider range of click chemistry strategies, such as sulfur(VI) fluoride exchange (SuFEx).[187–189]

Nucleophilic substitution reactions are widely employed for the post-polymerization biofunctionalization of polymer brushes,[190] leveraging the reactivity of typical monomers like dimethylaminoethyl methacrylate (DMAEMA), 2-(diethylamino)ethyl methacrylate (DEAEMA), and glycidyl methacrylate (GMA).[177] These reactions allow the introduction of functional groups, such as quaternary amines,[190] and azides.[176] For example, poly(GMA) can be functionalized with various nucleophiles, like amines,[4,191] thiols, and azides,[176] enabling diverse applications like enzyme[4] and DNA[191] immobilization.

Thiol–ene chemistry is increasingly applied in biomaterial biofunctionalization due to its compatibility with physiological conditions and photoactivation, making it suitable for selective reactions with peptides and proteins.[178,192,193] This method allows alkene-functionalized antifouling polymer brushes to be coupled with cell-adhesive peptides.[178] The light-triggered nature of thiol-ene chemistry also enables precise photopatterning designs, such as cell microarrays.[178,192,194] Functionalization is a fast process, usually taking about five minutes when using photo-irradiation. Its efficiency depends on the ratio between the thiol and the photoinitiator.[193] Thiol–yne reactions offer even higher thiol densities by allowing two thiol molecules to bind per alkyne site, enhancing surface functionality.[194,195]

The **alkyne – azide** cycloaddition, a 1,3-dipolar reaction between alkynes and azides, is widely used to biofunctionalize polymer brushes, forming 1,2,3-triazole adducts.[179,181,182] This reaction typically requires copper(I) catalysis, although strained alkynes like cyclo-octyne can react without a catalyst,[179,182] broadening its applications, especially in biological systems where metal toxicity is a concern. Copper catalysis increases efficiency but may pose issues due to toxic byproducts, prompting alternatives like copper protection or non-catalytic methods like ligands for copper protection.[196,197] Moreover, azide-containing monomers can be polymerized directly, allowing pre-functionalized polymer brushes, while other approaches

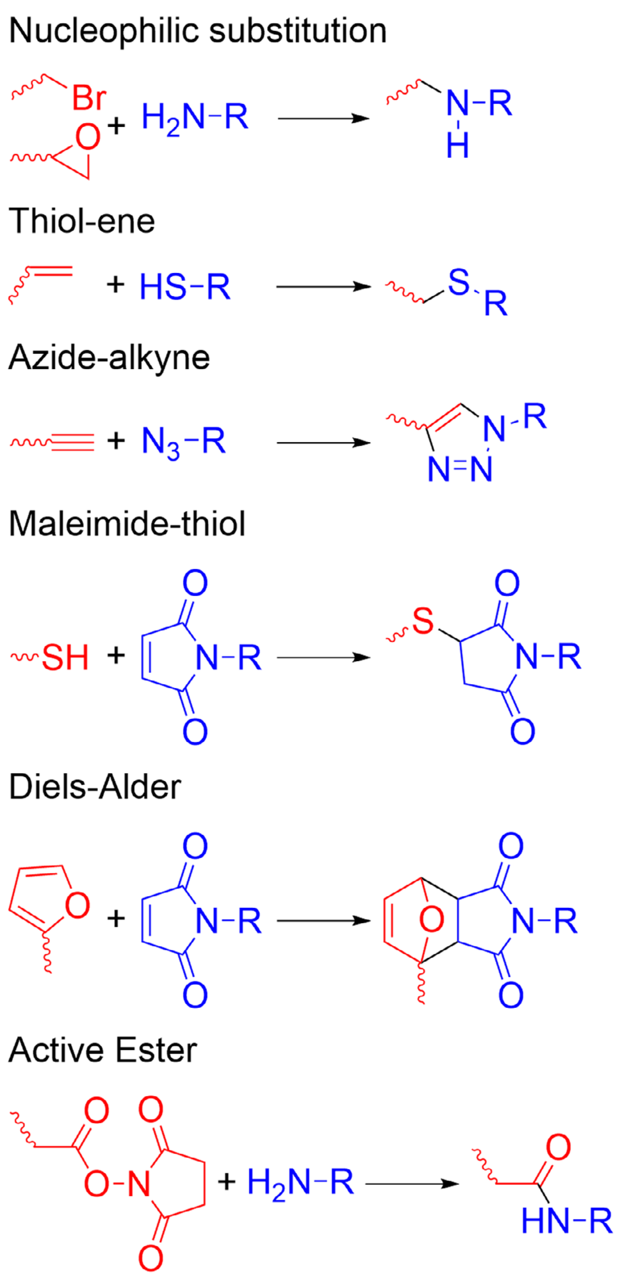

Figure 4. Different reactions can be utilized to couple biorecognition elements on the surfaces of polymer brushes. R indicates the biorecognition element, and 〰 indicates the polymer brush (note that in some cases the opposite is also possible).

require protecting and later deprotecting active groups for further modification.[180–182]

Maleimide-thiol coupling is a selective and efficient strategy for the biofunctionalization of polymer brushes, commonly used in bioconjugation.[183,198] In this reaction, maleimide groups on polymer brushes form stable covalent bonds with thiol groups, typically from cysteine residues in proteins or other molecules.[199] This reaction occurs rapidly under mild conditions, often at room temperature and physiological conditions, making it a good candidate for biological applications.[200] Maleimide-thiol coupling is favored for its specificity and ability to target thiols without affecting other functional groups.[201]

The **Diels–Alder** reaction is a well-established method for functionalizing polymer brushes, offering a robust way to introduce biospecific molecules[184] or other functional groups onto polymers.[202] This reaction is particularly valued for its high selectivity and mild reaction conditions.[70] The main drawback of this approach is that biospecific elements must be modified to incorporate the diene and dienophile into their structures.[70,181]

Due to its efficiency and versatility, **active ester** coupling is a widely used strategy for biofunctionalization of polymer brushes.[118,185,186,203,204] In this method, polymer brushes containing active ester groups, such as *N*-hydroxysuccinimide (NHS)[118,185,186,203,204] esters or pentafluorophenyl (PFP)[205] react readily with nucleophiles, allowing for the straightforward attachment of biomolecules like proteins,[29] peptides, antibodies,[185,186,205,206] or other biospecific molecules under mild conditions. Their high reactivity ensures fast coupling with minimal side reactions, making them ideal for creating functionalized surfaces in applications such as biosensing,[185,186] and tissue engineering.[174] Additionally, the reaction proceeds in aqueous or organic solvents, offering flexibility for different biomolecular systems.[207] Moreover, Lísalová et al. investigated further optimizing NHS group deactivation after coupling by applying glycine to poly(CBMAA)-NHS polymer brushes. This process restored the brushes' zwitterionic character, achieving a blood plasma fouling level of 51 ± 26 pg mm^{-2}.[185] This deactivation procedure was also applied in diblock structures consisting of poly(HPMA)-poly(CBMA) for deactivating the second block after coupling with an anti-fibrinogen monoclonal antibody.[204]

The biofunctionalization of polymer brushes can be achieved through four main approaches, each differing in how, and where, functional groups are introduced for coupling: chain-end,[70,181,206,208] side chain,[178,192] random copolymer,[118,185,186] and diblock[118,181,182,204] copolymer brush (**Figure 5**).

Chain-end biofunctionalization of polymer brushes offers several advantages. It allows precise placement of bioactive molecules at the terminal end of polymer chains, ensuring controlled availability and minimizing steric hindrance from the polymer brush.[70,181,206,208] This method can enhance the accessibility and functionality of biomolecules, improving interactions with target molecules in applications like biosensing.[70,181,206,208] However, chain-end functionalization often requires specific synthetic steps, making it more complex than random or side-chain functionalization.[70,206] Additionally, the density of biospecific groups is lower compared to functionalization along the entire polymer chain, which may limit the surface's overall bioactivity.[70,182]

Side-chain biofunctionalization of polymer brushes enables high-density attachment of biospecific molecules along the length of the polymer chains, increasing overall bioactivity and enhancing interactions in applications like biosensing or cell adhesion.[178,192] This approach also offers greater flexibility in tuning the spatial arrangement of functional groups. However, side-chain functionalization can lead to steric hindrance, potentially reducing the accessibility and effectiveness of the attached bioreceptor molecules.[209,210] Additionally, achieving uniform and controlled functionalization along the side chains may

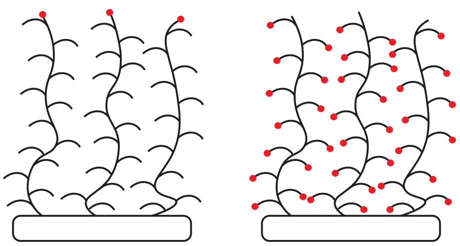

Figure 5. Various architectures for immobilizing biospecific elements on antifouling polymer brushes to create biospecific coatings.

require more complex chemistries. The increased surface crowding can also decrease the polymer brush's antifouling properties.[209]

Random copolymer brushes for biofunctionalization offer a versatile approach by incorporating multiple functional groups along the polymer backbone.[27,118,184–186] This allows for the simultaneous introduction of different biospecific molecules, enhancing multifunctionality and enabling complex biological interactions. Random copolymerization also simplifies the synthesis process, as biofunctional and non-biofunctional monomers are co-polymerized in a single step.[27,118,185,186] However, controlling the precise distribution and density of functional groups can be challenging, potentially leading to inconsistent bioactivity and relatively lower biospecific element immobilization.[118] Additionally, the random placement of functional groups may result in steric hindrance or reduced accessibility, impacting the biosensor performance.[118]

Diblock copolymer brushes for biofunctionalization offer precise spatial separation of functional groups, with one block dedicated to bioactivity and the other providing antifouling properties.[118,181,182,204] This allows for the controlled presentation of biospecific molecules in a well-organized manner, improving their accessibility and functionality, which is particularly useful in biosensing applications. The distinct block architecture can also enhance stability and reduce nonspecific protein interactions by limiting bioactivity to one block.[118,181,182,204] However, the synthesis of diblock copolymer brushes is more complex and often requires advanced polymerization techniques or multistep methods.[118,181,182]

Current developments in the biofunctionalization of polymer brushes use a wide variety of chemistries to couple biospecific biorecognition elements to antifouling polymer brushes. Nevertheless, active esters, particularly in NHS-EDC chemistry, probably remain the most commonly applied technique to immobilize biorecognition elements.[118,185,186,203,204] This is related to the wide presence of amine groups in almost any biospecific element and the relative simplicity of this approach. This attractive feature, however, is also one of the potential drawbacks, as it may lead to a wide variety of orientations of the biorecognition unit on the surface, with a concomitant reduction of the sensitivity of the device (see above for effects of orientation of, e.g., antibodies). Other approaches, such as azide-alkyne click chemistries, have a higher specificity and often preserve the structure of the biorecognition element.[153,181,182] These approaches frequently require post-polymerization modification of brush and biorecognition elements.[181,182] A wide variety of architectures can be used for the creation of biospecific surfaces.[174] The diblock system seems to be the most practical and balanced approach for creating biospecific layers, because of its high immobilization level of biorecognition elements on the second block and preserved antifouling properties at the first block.[118,181,182,204]

Polymer brushes may play a key role in stabilizing biomolecules attached to their surfaces. It is well known that attaching antibodies or aptamers directly to solid surfaces can lead to partial unfolding or a loss of function, especially when they adsorb onto bare materials. Hydrophobic or charged surface patches can denature proteins or aptamers upon contact.[211,212] Polymer brushes may help mitigate these effects through steric stabilization: the dense polymer chains act as a physical barrier between the bioreceptor and the solid substrate while also providing a solvent-rich cushion. Previous studies have shown that conjugation with bottlebrush polymers improves the stability of aptamers,[212] as does the use of polymer brush coatings.[213] The highly hydrated environment of polymer brushes may help in maintaining the native conformation of biomolecules by preventing exposure to dry or denaturing interfaces. This way, polymer brushes offer a "soft" landing pad, unlike hard surfaces.[214] This stabilizing effect may be further supported by the high performance of thrombin aptamer-based grating sensors incorporating poly(HPMA)-poly(CBMA) brushes, even in complex biological fluids such as blood serum.[215]

4. Applications of Biospecific Polymer Brushes in Biosensors

Biospecific polymer brush coatings have applications in various biosensing technologies.[6,27–28,210,215–217] Their unique ability to repel non-specific adsorption offers a significant advantage in label-free, high-sensitivity research techniques such as SPR (Surface Plasmon Resonance)[27,215,218] and QCMD (Quartz Crystal Microbalance with Dissipation monitoring).[6,28] The most commonly used coating in these systems is a poly[(*N*-(2-hydroxypropyl)-methacrylamide)-*co*-(carboxybetaine methacrylamide)] (poly(HPMAA-*co*-CBMAA)) random copolymer.[27,28,215–217] The biospecific element in such systems is typically attached through NHS/EDC active ester coupling with CBMAA moieties.[6,27,28,215]

4.1. Optical Biosensors

Combining polymer brushes with aptamer bioreceptors enables the analysis of medically relevant thrombin concentrations in

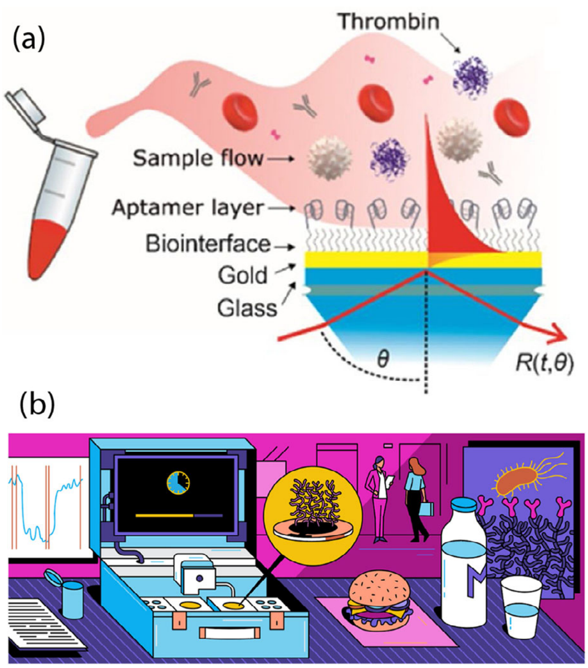

Figure 6. Examples of biosensor technologies a) Schematic of an antifouling SPR biosensor for direct thrombin detection in 10% human blood. The gold chip is coated with a polymer brush and thrombin-specific aptamers (HD1 short, HD1, HD22), enabling label-free, selective detection without sample pre-processing. Reproduced with permission.[27] Copyright 2020, Elsevier. b) A portable QCM biosensor with terpolymer brush nano-coatings enables rapid (30 min) and accurate detection of E. coli O157:H7 in real-world food samples. The sensor achieves low LODs (7.5 × 10^2 CFU mL^{-1} in milk, 3.1 × 10^3 CFU mL^{-1} in hamburgers, and 2.6 × 10^4 CFU mL^{-1} in dumplings) with high reusability over 60 sample injections. A custom-built four-channel portable system with an optimized microfluidic setup facilitates on-site analysis. Reproduced under terms of the CC-BY license.[28] Copyright 2024, Elsevier.

10% blood using a direct SPR detection format.[27] Furthermore, poly(HPMAA-*co*-CBMAA) coatings were applied to biosensors that detect hepatitis B antibodies in clinical saliva.[217] These coatings have found their application in biosensing food safety, detecting bacterial pathogens, like *E. coli*, in complex food samples.[28,145,216]

Recent developments have led to creation of a compact thrombin (coagulation factor II) sensor (**Figure 6**a).[27,215] This biosensor allows for direct, label-free detection of thrombin with aptamers in medically relevant concentrations (1–20 nM), without the need for sample dilution or additional signal enhancement.[215] Besides coagulation factor II, factor XII was also detected with an optical SPR sensor on functionalized poly(HPMAA-*co*-CBMAA) brushes with a C1-esterase inhibitor by the group of Rodriguez-Emmenegger.[150,151] They noticed that the inhibitor prevented factor XII, from being activated and therefore reduced coagulation of biomaterial on the surface even more.

4.2. Piezo Vibration-Based Biosensors

A sensor based on a triblock of poly(HPMAA-*ran*-CBMAA-*ran*-SBMAA) was applied to rapidly detect SARS-CoV-2 in clinical samples.[6] Similar terpolymer brushes have shown excellent antifouling properties with QCM in food samples, such as diluted milk and extractions from cheese and meat (Figure 6b).[28] Because of these antifouling properties, noise was decreased and a LOD of 2 CFU/mL was obtained for *S. aureus* binding to antibodies.[153,216]

4.3. Electrochemical Biosensors

Furthermore, a sandwich-type electrochemical immunosensor was successfully developed for the simultaneous and highly sensitive detection of PSA and AFP tumor markers.[219] Using a poly(acrylonitrile-g-glycidyl methacrylate) polymer brush loaded with Au nanoparticles for signal amplification, it achieved detection limits as low as 0.1 pg mL^{-1} (PSA) and 0.3 pg/mL (AFP) in single detection, and 2.2 pg mL^{-1} (PSA) and 1.8 pg mL^{-1} (AFP) in simultaneous detection. The sensor demonstrated high sensitivity, selectivity, and potential for clinical monitoring. The polymer brush coatings also serve as effective siRNA delivery systems, utilizing poly(DAMA-HEMA)-multilayered gold nanoparticles synthesized via surface-initiated ATRP.[220] The polymeric shells enable tunable siRNA loading, influencing cellular uptake and gene silencing. In a bioreductive environment, disulfide bonds break, releasing siRNA and significantly suppressing tumor growth in a murine lung carcinoma model.

It remains uncertain whether an optimal balance can be achieved by using zwitterionic brushes in electrochemical biosensors. While zwitterionic monolayers have shown a good trade-off between antifouling and sensitivity in biological fluids like FBS, increasing the coating thickness to a brush structure may reduce device sensitivity.[221] Self-assembled monolayers (SAMs) used as supports for polymer brushes act as dense, low-permittivity barriers that restrict ion and electroactive probe transport, behaving like pure capacitors in equivalent circuit models. Charge transfer through the SAM occurs via electron tunneling, which decreases exponentially with increasing SAM thickness.[222]

However, using electrically neutral yet highly polar, thin polymer brushes such as poly(HPMA) or poly(MeOEGMA) in the 5–15 nm range may offer a suitable compromise between antifouling performance and electrochemical responsiveness. Those brushes previously showed good antifouling performance at rather low thickness.[70,89] It also should be underscored that polymer brushes hold significant promise as highly effective antifouling coatings in Electrochemical Impedance Spectroscopy (EIS)-based biosensors, offering the potential to markedly reduce biofouling and improve sensor performance.[31]

5. Future Challenges and Prospects

The new approaches to synthesizing polymer brushes, such as SI-ARGET-ATRP,[104] SET-LRP, and PET-RAFT,[114,121] transform these biospecific coatings from purely lab-based to an applicable and scalable technology for diagnostics and point-of-care testing (POCT). Two POCT concepts to mention here are the “D4 assay” and the “D4-TFT assay”, which rely on SI-ATRP-prepared poly(HOEGMA) brushes for antibody and reagent immobilization, as described by Chilkoti et al.[223–224] Nevertheless, challenges may need to be addressed to integrate polymer brushes

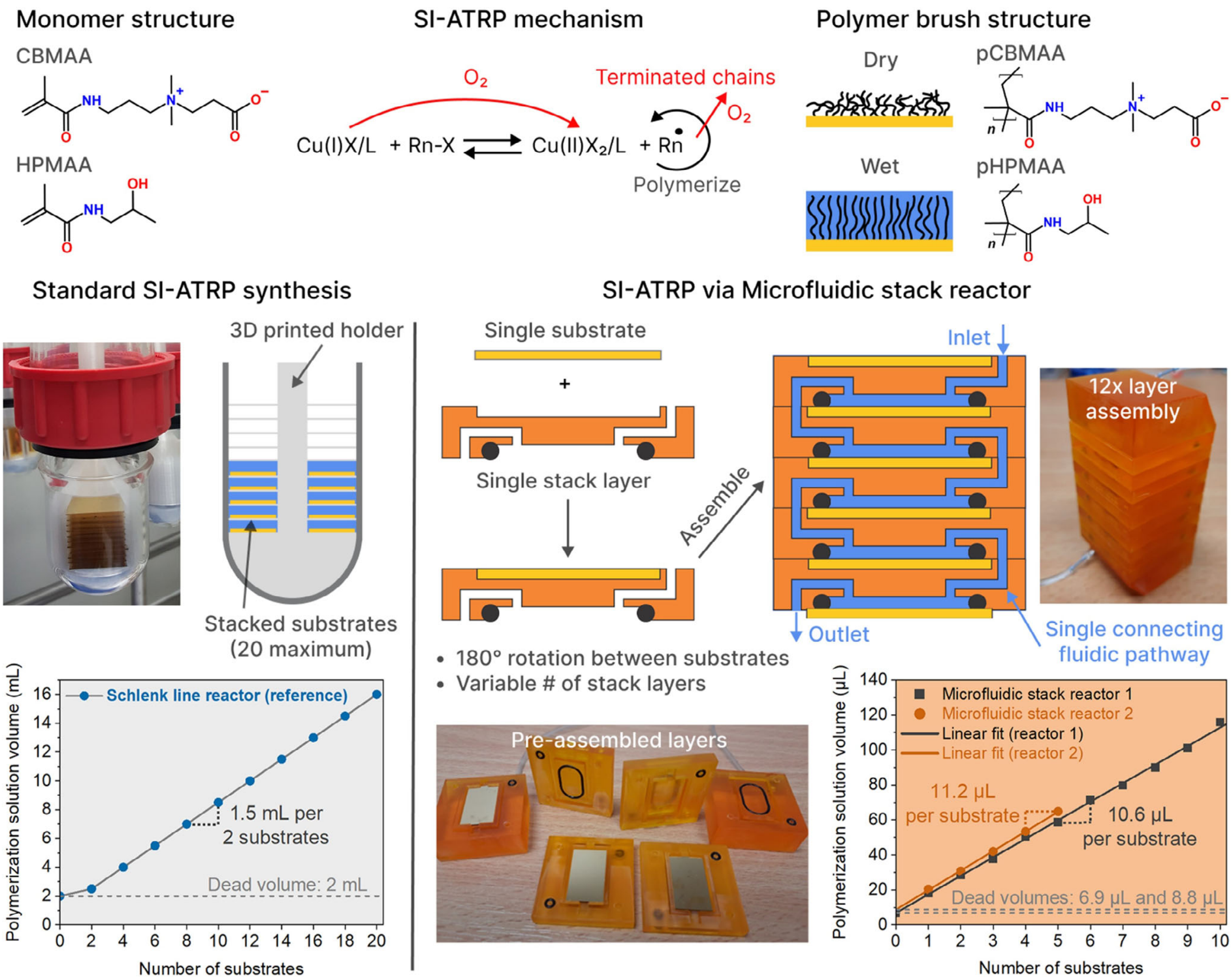

Figure 7. (top) Monomer structure, SI-ATRP mechanism, and the general structure of the PB films synthesized in this study; (bottom left) Examples and schematic of standard Schlenk line reactors (reference procedure); (bottom right) General schematic and design of the microfluidic stack reactors for SI-ATRP. Reproduced with permission.[128] Copyright 2025, Elsevier.

further into lab-based diagnostics and POCT. Such challenges are (1) full control and repeatability of polymer brush thickness and density on large substrates, (2) robust biofunctionalization strategies, and (3) less elaborate and multistep procedures to grow polymer brushes.[225] Lisalova et al. addressed these challenges by developing a microfluidic stack reactor, a 3D-printed, scalable system designed to significantly enhance polymerization efficiency—over 100-fold—while minimizing chemical consumption.[128] Using this reactor, they successfully synthesized high-quality polymer brushes with excellent antifouling properties. The results demonstrated that polymer brushes produced with this method were comparable, if not superior, to those synthesized through conventional techniques, highlighting the potential of this approach for efficient, large-scale polymer brush production (**Figure 7**).

Reliable large substrate modification with polymer brushes is essential for the analytical performance in certain biosensor concepts such as in SPR, photonic sensors, and electrochemical sensors. Therefore, precise control over layer thickness and brush density is essential. Initial work on wafer-scale applications of SI-PET-RAFT has been achieved.[69,226] Furthermore, wafer-scale SI-ATRP-grown polymer brushes have been successfully achieved by using a copper plate as a lid to confine the reaction volume. This versatile approach requires only a few µL of reagents, is oxygen-tolerant, and applies to various monomers.[227,228] Furthermore, when using SI-ARGET-ATRP, a glass cover can replace the copper plate, which was initially reported for poly(DMAEMA).[229] More recently, it has also been used to prepare wafer scale poly 3-sulfopropyl methacrylate (poly(SPMA)) brushes with ascorbic acid as the reducing agent.[104] Optimizing the reducing agent's concentration allows for the formation of a robust and uniform polymer brush at the full wafer scale.[104]

While polyethylene glycol (PEG)-based polymer brushes have been widely used, their long-term stability can be influenced by factors such as autooxidation upon oxygen exposure[230] However, recent studies by Lisalova[144] and Rodriguez-Emmenegger[22] highlight the superior stability of zwitterionic poly(CBMAA) and poly(HPMA) polymer brushes, which maintain their integrity over time, especially when stored in a dry state or in a buffer solution. These emerging polymer brush systems offer promising alternatives for long-lasting non-fouling surfaces. The grafted-from approach yields high-density brushes with optimal antifouling conditions. However, mass transport and charge transfer are limited in dense packed systems, which currently limits the application of these brushes in electrochemical biosensors.[146] A solution for this problem might be to use lower grafting densities (for example obtained from grafting-to strategies) and backfill the electrode surface with self-assembling molecules. Similar systems are currently used for aptamers[231–233] and peptides[234] that are grafted to gold electrodes, which are backfilled with mercapto-alkanols.[235]

The biofunctionalization route has to be stable and highly repeatable for scaling toward large substrates. NHS/EDC coupling chemistry is versatile, attractive, and probably the most commonly used routine, as it allows direct protein immobilization without any protein modification or conjugation.[185,186] However, in case of hydrolytic instability, more water-stable amino-reactive chemistries like epoxy or PFP for covalent coupling onto polymer brush-based biospecific surfaces could be explored.[236] An alternative route was presented by Chilkoti et al., who developed an elegant inkjet-printing-based noncovalent immobilization of antibodies onto SI-ATRP prepared poly(HOEGMA) polymer brushes, which greatly simplifies fabrication.[211,223,224] In this research antibodies were directly printed onto the poly(HOEGMA) layer, i.e., without any activation, and by a consecutive drying step under reduced pressure, the antibodies become noncovalently immobilized through entanglement in the poly(HOEGMA) brush layer. This method has no need for washing or blocking after immobilization and retains the antibodies' tertiary structure and activity. However, on zwitterionic poly(SBMA) this inkjet-printed noncovalent immobilization route failed due to the high hydrophilicity of the brush layer.[237] Therefore, a workaround was developed based on poly(2-dimethylaminoethyl) methacrylate (DMAEMA) brushes.[237] The hydrophilicity was tuned by derivatization of DMAEMA with iodoacetic acid into zwitterionic CBMA; this facilitated the noncovalent antibody immobilization and guaranteed excellent matrix-resistant properties.[237]

"Grafting-from" approaches based on SI-ATRP or SI-PET-RAFT are multistep chemistry protocols, including surface cleaning, initiator immobilization, synthesis of the polymer brush, extensive washing, activation or reactive group introduction, biofunctionalization, and washing. Reducing the number of steps would be desired to facilitate and boost the uptake of these high-performance surfaces in large-scale diagnostic lab-based and point-of-care testing applications. Alternatively, in-solution chemistry approaches may be applied in gas-phase procedures like initiated chemical vapor deposition (CVD). In iCVD an initiator molecule is thermally decomposed into free radicals. After adsorption onto (a cooled) surface gas phase, the polymerization of monomers proceeds. iCVD has developed into a solvent-free, very clean, versatile, and easily scalable process.[238,239] However, so far, it is limited to precursor molecules with a high enough vapor pressure.[240] This limits the direct use of zwitterionic, high-polarity, or high-molecular-weight precursors. Nevertheless, iCVD-based hydrophilic polymer brushes, like poly(HEMA),[238,241,242] poly(PVP),[243,244] and poly(HPMA)[239,245] have been reported. Limited studies on their antifouling properties have been reported.[244,246]

Reusing the (sensor) substrates, e.g., after the brush coating loses its functionality, is a sustainability challenge.[113] A possible solution is to completely remove the brush and initiators and refunctionalize afterward. Yet, this might involve hazardous chemicals such as HF,[247] strong acids,[248] bases,[249] or other chemicals.[250] A milder technique was recently demonstrated: Several types of polyester-based brushes were degraded under mild aqueous conditions and regrown repeatedly from the same initiator film.[111]

The introduction of diblock[118,181,182] and random[6,27,28,185,209,215,217] copolymer architectures for the biofunctionalization of polymer brushes allows the biofunctionalization unit to be spatially separated from the antifouling unit. Furthermore, they allow for high immobilization amounts of biospecific elements on the surface of polymer brushes and preserve their antifouling properties.[6,27,28,118,181,182,185,209,215,217] Combining this architecture with highly versatile chemistries allows the immobilization of almost any biospecific element on the surface of an antifouling polymer brush.[6,27,28,118,185,209,217] Therefore, it opens a path toward applying polymer brush coatings in biosensors that work in real undiluted biological liquids.[6,27,28,215–217] We envision the growth of polymer brush-based biospecific surfaces and their scalable applications in different fields, from biosensors to tissue engineering.

Acknowledgements

This publication is part of Targets 1 and 5 of the TTW Perspectief research program ReCoVR: Recovery and Circularity of Valuable Resources which is (partly) financed by the Dutch Research Council (NWO). This project has received funding from the research program Nationale Wetenschapsagenda – Onderzoek op Routes door Consortia (NWA-ORC) 2020/21, which was (partly) financed by the Dutch Research Council (NWO) under number NWA.1389.20.123 (to S.d. B.), from a Top-level Talent Project of Zhejiang Province (Jiaxing University, to H.Z.) and the affiliated universities. This project is made possible in part by a contribution from the National Growth Fund program NXTGEN Hightech.

Conflict of Interest

Luc Scheres is the CTO of Surfix B.V., a company focusing on point-of-care diagnostics for which biospecific surfaces are relevant.

Keywords

antifouling, biofunctionalization, biosensors, biospecific surfaces, fouling, polymer brushes

Received: November 28, 2024
Revised: April 15, 2025
Published online:

[1] Biosensors Market Size, Share, Growth Analysis, By Type (Sensor Patch, Embedded Devices), Product (Wearable, Non-Wearable),

Technology(Piezoelectric, Electrochemical, Thermal, Optical, Nanomechanical), Component, Application, End-User, and Region - Industry Forecast 2024-2031. Report ID: SQMIG45J2077, SkyQuest 2024.
[2] Biotechnology Market Size, Share & Trends Analysis Report By Technology (Nanobiotechnology, DNA Sequencing, Cell-based Assays), By Application (Health, Bioinformatics), By Region, And Segment Forecasts, 2023-2030. Report ID: 978-1-68038-134-4, Grand View Research Report **2023**.
[3] Biosensors Market Size, Share, Statistics, Industry Growth Analysis Report by Type, Product (Wearable, Non-Wearable), Technology, Application (POC, Home Diagnostics, Research Lab, Environmental Monitoring, Food & Beverages, Biodefense) Global Growth Driver and Industry Forecast to 2026. Report ID: SE 3097, Markets And Markets, **2021**.
[4] M. E. Welch, T. Doublet, C. Bernard, G. G. Malliaras, C. K. Ober, *J. Polym. Sci., Part A: Polym. Chem.* **2015**, *53*, 372.
[5] G. Pasternak, J. Greenman, I. Ieropoulos, *Sens. Actuators, B* **2017**, *244*, 815.
[6] M. Forinová, A. Pilipenco, I. Víšová, J. Kunčák, N. S. Lynn, P. Yudin, J. Dostálek, V. Hönig, M. Palus, H. Mašková, F. Dyčka, J. Štěrba, M. Vrabcová, J. Arnoštová, M. Spasovová, C. P. Tung, A. S. Yang, A. Dejneka, H. Vaisocherová-Lísalová, presented at 2021 IEEE Sensors **2021**.
[7] S. Kurbanoglu, C. Erkmen, B. Uslu, *TrAC, Trends Anal. Chem.* **2020**, *124*, 115809.
[8] J. Kim, A. S. Campbell, B. E. de Avila, J. Wang, *Nat. Biotechnol.* **2019**, *37*, 389.
[9] P. Mohankumar, J. Ajayan, T. Mohanraj, R. Yasodharan, *Measurement* **2021**, *167*, 108293.
[10] A. K. Singh, S. Mittal, M. Das, A. Saharia, M. Tiwari, *Alexandria Eng. J.* **2023**, *67*, 673.
[11] Y. Wang, K. Jia, J. Lin, *TrAC, Trends Anal. Chem.* **2024**, *177*, 117785.
[12] B. Kaur, S. Kumar, B. K. Kaushik, *Biosens. Bioelectron.* **2022**, *197*, 113805.
[13] A. Uniyal, G. Srivastava, A. Pal, S. Taya, A. Muduli, *Plasmonics* **2023**, *18*, 735.
[14] K. H. G. Fahad Usman, Y. Wing Fen, F. Meriaudeau, R. Jose, *Eur. Polym. J.* **2023**, *195*, 112250.
[15] J. U. Lee, W. H. Kim, H. S. Lee, K. H. Park, S. J. Sim, *Small* **2019**, *15*, 1804968.
[16] E. R. Kim, C. Joe, R. J. Mitchell, M. B. Gu, *Trends Biotechnol.* **2023**, *41*, 374.
[17] Y. Lee, K. Choi, J. E. Kim, S. Cha, J. M. Nam, *ACS Nano* **2024**, *18*, 25359.
[18] D. Murugan, M. Tintelott, M. S. Narayanan, X.-T. Vu, T. Kurkina, C. Rodriguez-Emmenegger, U. Schwaneberg, J. Dostalek, S. Ingebrandt, V. Pachauri, *Adv. Opt. Mater.* **2024**, *12*, 2401862.
[19] V. Yesudasu, H. S. Pradhan, R. J. Pandya, *Heliyon* **2021**, *7*, 06321.
[20] R. H. Ritchie, *Phys. Rev.* **1957**, *106*, 874.
[21] E. Kretschmann, H. Raether, **1968**, *23*, 2135.
[22] C. Rodriguez-Emmenegger, E. Brynda, T. Riedel, M. Houska, V. Šubr, A. B. Alles, E. Hasan, J. E. Gautrot, W. T. S. Huck, *Macromol. Rapid Commun.* **2011**, *32*, 952.
[23] D. Barchiesi, T. Grosges, F. Colas, M. L. D. L. Chapelle, *J. Opt. (U K)* **2015**, *17*, 114009.
[24] S. A. Meyer, E. C. Le Ru, P. G. Etchegoin, *Anal. Chem.* **2011**, *83*, 2337.
[25] T. E. Alexander, L. D. Lozeau, T. A. Camesano, *Cell Surface* **2019**, *5*, 100024.
[26] F. Bonyadi, M. Kavruk, S. Ucak, B. Cetin, G. Bayramoglu, A. D. Dursun, Y. Arica, V. C. Ozalp, *Crit. Rev. Anal. Chem.* **2023**, *54*, 2888.
[27] D. Kotlarek, F. Curti, M. Vorobii, R. Corradini, M. Careri, W. Knoll, C. Rodriguez-Emmenegger, J. Dostálek, *Sens. Actuators, B* **2020**, *320*, 128380.
[28] M. Forinová, A. Pilipenco, N. S. Lynn, R. Obořilová, H. Šimečková, M. Vrabcová, M. Spasovová, R. Jack, P. Horák, M. Houska, P. Skládal, P. Šedivák, Z. Farka, H. Vaisocherová-Lísalová, *Food Control* **2024**, *165*, 110695.
[29] M. Wang, Y. Yang, J. Min, Y. Song, J. Tu, D. Mukasa, C. Ye, C. Xu, N. Heflin, J. S. McCune, T. K. Hsiai, Z. Li, W. Gao, *Nat. Biomed. Eng.* **2022**, *6*, 1225.
[30] C. Zhang, S. Zhang, Y. Jia, Y. Li, P. Wang, Q. Liu, Z. Xu, X. Li, Y. Dong, *Biosens. Bioelectron.* **2019**, *126*, 785.
[31] J. Anthi, V. Kolivoska, B. Holubova, H. Vaisocherova-Lisalova, *Biomater. Sci.* **2021**, *9*, 7379.
[32] Y. Yang, Q. Yan, Q. Liu, Y. Li, H. Liu, P. Wang, L. Chen, D. Zhang, Y. Li, Y. Dong, *Biosens. Bioelectron.* **2018**, *99*, 450.
[33] J. J. García-Guzmán, J. M. Jiménez Heras, D. López-Iglesias, R. J. González-Álvarez, L. Cubillana-Aguilera, C. González Macías, J. J. Fernández Alba, J. M. Palacios-Santander, *Microchim. Acta* **2024**, *191*, 526.
[34] P. Samadi Pakchin, H. Ghanbari, R. Saber, Y. Omidi, *Biosens. Bioelectron.* **2018**, *122*, 68.
[35] N. Djellouli, M. Rochelet-Dequaire, B. Limoges, M. Druet, P. Brossier, *Biosens. Bioelectron.* **2007**, *22*, 2906.
[36] P. S. Pakchin, S. A. Nakhjavani, R. Saber, H. Ghanbari, Y. Omidi, *TrAC, Trends Anal. Chem.* **2017**, *92*, 32.
[37] H. Zhang, Q. Lu, F. Zuo, R. Yuan, S. Chen, *Sens. Actuators, B* **2017**, *241*, 887.
[38] P. E. Molinari, A. R. Krapp, A. Weiner, H. M. Beyer, A. K. Kondadi, T. Blomeier, M. López, P. Bustos-Sanmamed, E. Tevere, W. Weber, A. S. Reichert, N. B. Calcaterra, M. Beller, N. Carrillo, M. D. Zurbriggen, *Nat. Commun.* **2023**, *14*, 3277.
[39] M. Scherschel, J.-O. Niemeier, L. J. H. C. Jacobs, M. D. A. Hoffmann, A. Diederich, C. Bell, P. Höhne, S. Raetz, J. B. Kroll, J. Steinbeck, S. Lichtenauer, J. Multhoff, J. Zimmermann, T. Sadhanasatish, R. A. Rothemann, C. Grashoff, J. Messens, E. Ampofo, M. W. Laschke, J. Riemer, L. P. Roma, M. Schwarzländer, B. Morgan, *Nat. Commun.* **2024**, *15*, 10704.
[40] S. Bu, K. Wang, Z. Li, C. Wang, Z. Hao, W. Liu, J. Wan, *Analyst* **2020**, *145*, 4328.
[41] K. Yamashita, T. Shimizu, S. Shingubara, H. Ishida, A. Kuzuya, T. Ito, presented at 2024 IEEE SENSORS October, **2024**.
[42] D. Kang, F. Ricci, R. J. White, K. W. Plaxco, *Anal. Chem.* **2016**, *88*, 10452.
[43] M. Chen, R. Han, Y. Li, X. Luo, *Anal. Chim. Acta* **2022**, *1224*, 340191.
[44] D. Sadighbayan, M. Hasanzadeh, E. Ghafar-Zadeh, *TrAC, Trends Anal. Chem.* **2020**, *133*, 116067.
[45] J. S. Daniels, N. Pourmand, *Electroanalysis* **2007**, *19*, 1239.
[46] S. Arman, R. D. Tilley, J. J. Gooding, *Analyst* **2024**, *149*, 269.
[47] A. Hucknall, S. Rangarajan, A. Chilkoti, *Adv. Mater.* **2009**, *21*, 2441.
[48] A. d. l. S. Pereira, C. Rodriguez-Emmenegger, F. Surman, T. Riedel, A. B. Alles, E. Brynda, *RSC Adv.* **2014**, *4*, 2318.
[49] J. Baggerman, M. M. J. Smulders, H. Zuilhof, *Langmuir* **2019**, *35*, 1072.
[50] S. Szunerits, Q. Pagneux, Y. B. M'Barek, S. Vassal, R. Boukherroub, *Bioelectrochemistry* **2023**, *153*, 108479.
[51] M. J. Russo, M. Han, P. E. Desroches, C. S. Manasa, J. Dennaoui, A. F. Quigley, R. M. I. Kapsa, S. E. Moulton, R. M. Guijt, G. W. Greene, S. M. Silva, *ACS Sens.* **2021**, *6*, 1482.
[52] C. Jiang, G. Wang, R. Hein, N. Liu, X. Luo, J. J. Davis, *Chem. Rev.* **2020**, *120*, 3852.
[53] N. Erathodiyil, H.-M. Chan, H. Wu, J. Y. Ying, *Mater. Today* **2020**, *38*, 84.
[54] J. D. Andrade, V. L. Hlady, R. A. van Wagenen, *Pure Appl. Chem.* **1984**, *56*, 1345.
[55] P. A. Fritz, B. Bera, J. van den Berg, I. Visser, J. M. Kleijn, R. M. Boom, C. G. P. H. Schroën, *Langmuir* **2021**, *37*, 6549.

[56] L. Vroman, A. L. Adams, *Surf. Sci.* **1969**, *16*, 438.
[57] S. L. Hirsh, D. R. McKenzie, N. J. Nosworthy, J. A. Denman, O. U. Sezerman, M. M. M. Bilek, *Colloids Surf., B* **2013**, *103*, 395.
[58] M. Rabe, D. Verdes, S. Seeger, *Adv. Colloid Interface Sci.* **2011**, *162*, 87.
[59] C. Boo, S. Hong, M. Elimelech, *Environ. Sci. Technol.* **2018**, *52*, 14198.
[60] P. Harder, M. Grunze, R. Dahint, G. M. Whitesides, P. E. Laibinis, *J. Phys. Chem. B* **1998**, *102*, 426.
[61] F. Wang, H. Zhang, B. Yu, S. Wang, Y. Shen, H. Cong, *Prog. Org. Coat.* **2020**, *147*, 105860.
[62] S. P. Pujari, L. Scheres, A. T. M. Marcelis, H. Zuilhof, *Angew. Chem., Int. Ed.* **2014**, *53*, 6322.
[63] A. de los Santos Pereira, T. Riedel, E. Brynda, C. Rodriguez-Emmenegger, *Sens. Actuators, B* **2014**, *202*, 1313.
[64] X. Xu, Y. Chang, Y. Gong, Y. Zhang, Y. Yu, H. Peng, C. Fu, *ACS Appl. Polym. Mater* **2024**, *6*, 1.
[65] Y. Hu, B. Liang, L. Fang, G. Ma, G. Yang, Q. Zhu, S. Chen, X. Ye, *Langmuir* **2016**, *32*, 11763.
[66] Z. Ding, C. Chen, Y. Yu, S. de Beer, *J. Mater. Chem. B* **2022**, *10*, 2430.
[67] M. Kobayashi, Y. Terayama, H. Yamaguchi, M. Terada, D. Murakami, K. Ishihara, A. Takahara, *Langmuir* **2012**, *28*, 7212.
[68] H. Ji, P. G. De Gennes, *Macromolecules* **1993**, *26*, 520.
[69] A. R. Kuzmyn, L. W. Teunissen, M. V. Kroese, J. Kant, S. Venema, H. Zuilhof, *ACS Omega* **2022**, *7*, 38371.
[70] A. R. Kuzmyn, A. de los Santos Pereira, O. Pop-Georgievski, M. Bruns, E. Brynda, C. Rodriguez-Emmenegger, *Polym. Chem.* **2014**, *5*, 4124.
[71] M. D. M. E. Linssen, Y.-T. Lin, S. A. H. van den Wildenberg, M. M. E. Tholen, A. M. de Jong, M. W. J. Prins, *Bioconjugate Chem.* **2024**, *35*, 996.
[72] A. Kopyshev, K. Kanevche, N. Lomadze, E. Pfitzner, S. Loebner, R. R. Patil, J. Genzer, J. Heberle, S. Santer, *ACS Appl. Polym. Mater* **2019**, *1*, 3017.
[73] A. R. Kuzmyn, T. G. Ypma, H. Zuilhof, *Langmuir* **2024**, *40*, 3354.
[74] I. Víšová, B. Smolková, M. Uzhytchak, M. Vrabcová, Y. Zhigunova, M. Houska, F. Surman, A. de los Santos Pereira, O. Lunov, A. Dejneka, H. Vaisocherová-Lísalová, *Macromol. Biosci.* **2020**, *20*, 1900351.
[75] W. Yan, S. N. Ramakrishna, M. Romio, E. M. Benetti, *Langmuir* **2019**, *35*, 13521.
[76] K. J. van der Weg, G. C. Ritsema van Eck, S. de Beer, *Lubricants* **2019**, *7*, 84.
[77] E. M. Benetti, N. D. Spencer, *Helv. Chim. Acta* **2019**, *102*, 1900071.
[78] A. R. Kuzmyn, I. Stokvisch, G.-J. Linker, J. M. J. Paulusse, S. de Beer, *ACS Appl. Polym. Mater* **2025**, *7*, 3842.
[79] V. Escobar, N. Scaramozzino, J. Vidic, A. Buhot, R. Mathey, C. Chaix, Y. Hou, *Biosensors* **2023**, *13*, 258.
[80] A. K. Trilling, T. Hesselink, A. v. Houwelingen, J. H. G. Cordewener, M. A. Jongsma, S. Schoffelen, J. C. M. v. Hest, H. Zuilhof, J. Beekwilder, *Biosens. Bioelectron.* **2014**, *60*, 130.
[81] A. K. Trilling, J. Beekwilder, H. Zuilhof, *Analyst* **2013**, *138*, 1619.
[82] B. Saha, T. H. Evers, M. W. J. Prins, *Anal. Chem.* **2014**, *86*, 8158.
[83] B. Saha, P. Songe, T. H. Evers, M. W. J. Prins, *Analyst* **2017**, *142*, 4247.
[84] M. Henze, D. Mädge, O. Prucker, J. Rühe, *Macromolecules* **2014**, *47*, 2929.
[85] M. M. Avdeev, A. V. Shibaev, K. I. Maslakov, S. V. Dvoryak, B. V. Lokshin, Y. E. Gorshkova, T. V. Tropin, O. E. Philippova, *Langmuir* **2024**, *40*, 23918.
[86] E. Roeven, A. R. Kuzmyn, L. Scheres, J. Baggerman, M. M. J. Smulders, H. Zuilhof, *Langmuir* **2020**, *36*, 10187.
[87] L. W. Teunissen, J. van den Beukel, M. M. J. Smulders, H. Zuilhof, *Adv. Mater. Interfaces* **2022**, *9*, 2201198.
[88] S. Dedisch, F. Obstals, A. de los Santos Pereira, M. Bruns, F. Jakob, U. Schwaneberg, C. Rodriguez-Emmenegger, *Adv. Mater. Interfaces* **2019**, *6*, 1900847.
[89] Y.-M. Wang, A. Kálosi, Y. Halahovets, I. Romanenko, J. Slabý, J. Homola, J. Svoboda, A. de los Santos Pereira, O. Pop-Georgievski, *Polym. Chem.* **2022**, *13*, 3815.
[90] E. M. Benetti, M. Divandari, S. N. Ramakrishna, G. Morgese, W. Yan, L. Trachsel, *Chem.-Eur. J.* **2017**, *23*, 12433.
[91] L. Li, B. Yan, L. Zhang, Y. Tian, H. Zeng, *Chem. Commun.* **2015**, *51*, 15780.
[92] M. Schroffenegger, N. S. Leitner, G. Morgese, S. N. Ramakrishna, M. Willinger, E. M. Benetti, E. Reimhult, *ACS Nano* **2020**, *14*, 12708.
[93] C. Feng, X. Huang, *Acc. Chem. Res.* **2018**, *51*, 2314.
[94] B. Xu, C. Feng, Y. Lv, S. Lin, G. Lu, X. Huang, *ACS Appl. Mater. Interfaces* **2020**, *12*, 1588.
[95] C. Yoshikawa, R. Takagi, T. Nakaji-Hirabayashi, T. Ochi, Y. Kawamura, H. Thissen, *ACS Appl. Mater. Interfaces* **2022**, *14*, 32497.
[96] L. W. Teunissen, M. M. J. Smulders, H. Zuilhof, *Adv. Mater. Interfaces* **2023**, *10*, 2202503.
[97] K. Matyjaszewski, *Macromolecules* **2012**, *45*, 4015.
[98] N. P. Truong, G. R. Jones, K. G. E. Bradford, D. Konkolewicz, A. Anastasaki, *Nat. Rev. Chem.* **2021**, *5*, 859.
[99] J.-S. Wang, K. Matyjaszewski, *J. Am. Chem. Soc.* **1995**, *117*, 5614.
[100] R. Wang, Q. Wei, W. Sheng, B. Yu, F. Zhou, B. Li, *Angew. Chem., Int. Ed.* **2023**, *62*, 202219312.
[101] K. Matyjaszewski, J. Xia, *Chem. Rev.* **2001**, *101*, 2921.
[102] K. Matyjaszewski, *Eur. Polym. J.* **2024**, *211*, 113001.
[103] W. Jakubowski, K. Min, K. Matyjaszewski, *Macromolecules* **2006**, *39*, 39.
[104] L. B. Veldscholte, S. de Beer, *ACS Appl. Polym. Mater* **2023**, *5*, 7652.
[105] L. A. Navarro, A. E. Enciso, K. Matyjaszewski, S. Zauscher, *J. Am. Chem. Soc.* **2019**, *141*, 3100.
[106] G. Szczepaniak, L. Fu, H. Jafari, K. Kapil, K. Matyjaszewski, *Acc. Chem. Res.* **2021**, *54*, 1779.
[107] X. Hu, G. Szczepaniak, A. Lewandowska-Andralojc, J. Jeong, B. Li, H. Murata, R. Yin, A. M. Jazani, S. R. Das, K. Matyjaszewski, *J. Am. Chem. Soc.* **2023**, *145*, 24315.
[108] D. J. Siegwart, M. Leiendecker, R. Langer, D. G. Anderson, *Macromolecules* **2012**, *45*, 1254.
[109] D. Hong, H.-C. Hung, K. Wu, X. Lin, F. Sun, P. Zhang, S. Liu, K. E. Cook, S. Jiang, *ACS Appl. Mater. Interfaces* **2017**, *9*, 9255.
[110] D. Konkolewicz, Y. Wang, P. Krys, M. Zhong, A. A. Isse, A. Gennaro, K. Matyjaszewski, *Polym. Chem.* **2014**, *5*, 4409.
[111] M. Brió Pérez, M. A. Hempenius, S. de Beer, F. R. Wurm, *Macromolecules* **2023**, *56*, 8856.
[112] M. B. Pérez, D. A. Resendiz-Lara, Y. Matsushita, S. Kakinoki, Y. Iwasaki, M. A. Hempenius, S. de Beer, F. R. Wurm, *Adv. Funct. Mater.* **2024**, *34*, 2316201.
[113] M. Brió Pérez, F. R. Wurm, S. de Beer, *Langmuir* **2024**, *40*, 7249.
[114] A. R. Kuzmyn, A. T. Nguyen, L. W. Teunissen, H. Zuilhof, J. Baggerman, *Langmuir* **2020**, *36*, 4439.
[115] S. Perrier, *Macromolecules* **2017**, *50*, 7433.
[116] D. Zhou, E. Mastan, S. Zhu, *Macromol. Theory Simul.* **2012**, *21*, 602.
[117] M. Zamfir, C. Rodriguez-Emmenegger, S. Bauer, L. Barner, A. Rosenhahn, C. Barner-Kowollik, *J. Mater. Chem. B* **2013**, *1*, 6027.
[118] A. R. Kuzmyn, L. W. Teunissen, P. Fritz, B. van Lagen, M. M. J. Smulders, H. Zuilhof, *Adv. Mater. Interfaces* **2022**, *9*, 2101784.
[119] J. Xu, S. Shanmugam, H. T. Duong, C. Boyer, *Polym. Chem.* **2015**, *6*, 5615.
[120] M. L. Allegrezza, D. Konkolewicz, *ACS Macro Lett.* **2021**, *10*, 433.
[121] A. R. Kuzmyn, M. van Galen, B. van Lagen, H. Zuilhof, *Polym. Chem.* **2023**, *14*, 3357.

[122] S. E. Seo, E. H. Discekici, Y. Zhang, C. M. Bates, C. J. Hawker, *J. Polym. Sci.* **2020**, *58*, 70.
[123] J. Niu, D. J. Lunn, A. Pusuluri, J. I. Yoo, M. A. O'Malley, S. Mitragotri, H. T. Soh, C. J. Hawker, *Nat. Chem.* **2017**, *9*, 537.
[124] T. Lueckerath, T. Strauch, K. Koynov, C. Barner-Kowollik, D. Y. W. Ng, T. Weil, *Biomacromolecules* **2019**, *20*, 212.
[125] Z. Riedelová, A. de los Santos Pereira, J. Svoboda, O. Pop-Georgievski, P. Májek, K. Pečánková, F. Dyčka, C. Rodriguez-Emmenegger, T. Riedel, *Macromol. Biosci.* **2022**, *22*, 2200247.
[126] K. Matyjaszewski, N. V. Tsarevsky, *Nat. Chem.* **2009**, *1*, 276.
[127] M. Fromel, D. M. Sweeder, S. Jang, T. A. Williams, S. H. Kim, C. W. Pester, *ACS Appl. Polym. Mater* **2021**, *3*, 5291.
[128] M. Vrabcová, M. Spasovová, V. Cirik, J. Anthi, A. Pilipenco, M. Houska, O. Romanyuk, H. Vaisocherová-Lísalová, N. Scott Lynn, *Chem. Eng. J.* **2025**, *508*, 160914.
[129] O. Pop-Georgievski, C. Rodriguez-Emmenegger, A. d. l. S. Pereira, V. Proks, E. Brynda, F. Rypáček, *J. Mater. Chem. B* **2013**, *1*, 2859.
[130] F. Sun, K. Wu, H.-C. Hung, P. Zhang, X. Che, J. Smith, X. Lin, B. Li, P. Jain, Q. Yu, S. Jiang, *Anal. Chem.* **2017**, *89*, 10999.
[131] F. K. Metze, H.-A. Klok, *Macromolecules* **2025**, *58*, 3554.
[132] C. Yoshikawa, S. Hattori, C.-F. Huang, H. Kobayashi, M. Tanaka, *J. Mater. Chem. B* **2021**, *9*, 5794.
[133] T. Riedel, A. de los Santos Pereira, J. Táborská, Z. Riedelová, O. Pop-Georgievski, P. Májek, K. Pečánková, C. Rodriguez-Emmenegger, *Macromol. Biosci.* **2022**, *22*, 2100460.
[134] I. Víšová, M. Vrabcová, M. Forinová, Y. Zhigunová, V. Mironov, M. Houska, E. Bittrich, K.-J. Eichhorn, H. Hashim, P. Schovánek, A. Dejneka, H. Vaisocherová-Lísalová, *Langmuir* **2020**, *36*, 8485.
[135] J. Englert, M. Palà, L. Witzdam, F. Rayatdoost, O. Grottke, G. Lligadas, C. Rodriguez-Emmenegger, *Langmuir* **2023**, *39*, 18476.
[136] J. Englert, L. Witzdam, D. Söder, M. Garay-Sarmiento, A. Joseph, A. M. Wagner, C. Rodriguez-Emmenegger, *Macromol. Chem. Phys.* **2023**, *224*, 2300306.
[137] P. Tang, S. di Cio, W. Wang, J. E. Gautrot, *Langmuir* **2018**, *34*, 10019.
[138] X. Xu, X. Huang, Y. Chang, Y. Yu, J. Zhao, N. Isahak, J. Teng, R. Qiao, H. Peng, C.-X. Zhao, T. P. Davis, C. Fu, A. K. Whittaker, *Biomacromolecules* **2021**, *22*, 330.
[139] Z. Riedelová, A. de los Santos Pereira, D. F. Dorado Daza, P. Májek, F. Dyčka, T. Riedel, *Macromol. Biosci.* **2024**, *24*, 2300558.
[140] L. W. Teunissen, A. R. Kuzmyn, F. S. Ruggeri, M. M. J. Smulders, H. Zuilhof, *Adv. Mater. Interfaces* **2022**, *9*, 2101717.
[141] M. Singh, L. Poláková, A. de los Santos Pereira, O. Pop-Georgievski, J. Svoboda, T. Riedel, S. Gupta, Z. Sedláková, V. Raus, R. Poręba, *Polym. Chem.* **2024**, *15*, 3300.
[142] P. Wang, Y. Dong, S. Zhang, W. Liu, Z. Wu, H. Chen, *Colloids Surf., B* **2019**, *177*, 448.
[143] C. J. Reese, Y. Qi, D. T. Abele, M. J. Wagner, X. Liu, S. G. Boyes, *ACS Appl. Polym. Mater* **2022**, *4*, 1890.
[144] M. Vrabcová, M. Spasovová, M. Houska, K. Mrkvová, N. S. Lynn, L. Fekete, O. Romanyuk, A. Dejneka, H. Vaisocherová-Lísalová, *Prog. Org. Coat.* **2024**, *188*, 108187.
[145] I. Víšová, M. Houska, M. Spasovová, M. Forinová, A. Pilipenco, K. Mezuláníková, M. Tomandlová, K. Mrkvová, M. Vrabcová, A. Dejneka, J. Dostálek, H. Vaisocherová-Lísalová, *Adv. Mater. Interfaces* **2022**, *9*, 2201210.
[146] J. Anthi, E. Vaněčková, M. Spasovová, M. Houska, M. Vrabcová, E. Vogelová, B. Holubová, H. Vaisocherová-Lísalová, V. Kolivoška, *Anal. Chim. Acta* **2023**, *1276*, 341640.
[147] X.-Y. Zhang, Y.-Q. Zhao, Y. Zhang, A. Wang, X. Ding, Y. Li, S. Duan, X. Ding, F.-J. Xu, *Biomacromolecules* **2019**, *20*, 4171.
[148] Z. Zhou, Q. Shi, *Polymers* **2024**, *16*, 1634.
[149] Q. Ye, B. He, Y. Zhang, J. Zhang, S. Liu, F. Zhou, *ACS Appl. Mater. Interfaces* **2019**, *11*, 39171.
[150] J. Quandt, M. Garay-Sarmiento, L. Witzdam, J. Englert, Y. Rutsch, C. Stöcker, F. Obstals, O. Grottke, C. Rodriguez-Emmenegger, *Adv. Mater. Interfaces* **2022**, *9*, 2201055.
[151] L. Witzdam, B. Vosberg, K. Große-Berkenbusch, S. Stoppelkamp, H. P. Wendel, C. Rodriguez-Emmenegger, *Macromol. Biosci.* **2024**, *24*, 2300321.
[152] M. Forinová, A. Pilipenco, I. Víšová, N. S. Lynn Jr., J. Dostálek, H. Mašková, V. Hönig, M. Palus, M. Selinger, P. Kočová, F. Dyčka, J. Štěrba, M. Houska, M. Vrabcová, P. Horák, J. Anthi, C.-P. Tung, C.-M. Yu, C.-Y. Chen, Y.-C. Huang, P.-H. Tsai, S.-Y. Lin, H.-J. Hsu, A.-S. Yang, A. Dejneka, H. Vaisocherová-Lísalová, *ACS Appl. Mater. Interfaces* **2021**, *13*, 60612.
[153] M. Vorobii, R. Teixeira-Santos, L. C. Gomes, M. Garay-Sarmiento, A. M. Wagner, F. J. Mergulhão, C. Rodriguez-Emmenegger, *Prog. Org. Coat.* **2022**, *163*, 106609.
[154] Q. Wu, S. Guo, X. Liang, W. Sun, J. Lei, L. Pan, X. Liu, H. Chen, *Biomacromolecules* **2024**, *25*, 7202.
[155] C. Zhao, L. Li, Q. Wang, Q. Yu, J. Zheng, *Langmuir* **2011**, *27*, 4906.
[156] J. Yang, M. Zhang, H. Chen, Y. Chang, Z. Chen, J. Zheng, *Biomacromolecules* **2014**, *15*, 2982.
[157] E. van Andel, S. C. Lange, S. P. Pujari, E. J. Tijhaar, M. M. J. Smulders, H. F. J. Savelkoul, H. Zuilhof, *Langmuir* **2019**, *35*, 1181.
[158] H. Vaisocherová, Z. Zhang, W. Yang, Z. Cao, G. Cheng, A. D. Taylor, M. Piliarik, J. Homola, S. Jiang, *Biosens. Bioelectron.* **2009**, *24*, 1924.
[159] P. Sarker, T. Lu, D. Liu, G. Wu, H. Chen, M. S. Jahan Sajib, S. Jiang, Z. Chen, T. Wei, *Chem. Sci.* **2023**, *14*, 7500.
[160] B. Li, P. Jain, J. Ma, J. K. Smith, Z. Yuan, H.-C. Hung, Y. He, X. Lin, K. Wu, J. Pfaendtner, S. Jiang, *Sci. Adv.* **2019**, *5*, aaw9562.
[161] R. Konradi, C. Acikgoz, M. Textor, *Macromol. Rapid Commun.* **2012**, *33*, 1663.
[162] B. Pidhatika, M. Rodenstein, Y. Chen, E. Rakhmatullina, A. Mühlebach, C. Acikgöz, M. Textor, R. Konradi, *Biointerphases* **2012**, *7*, 1.
[163] C. W. Pester, H.-A. Klok, E. M. Benetti, *Macromolecules* **2023**, *56*, 9915.
[164] T. Li, H. Li, H. Wang, W. Lu, M. Osa, Y. Wang, J. Mays, K. Hong, *Polymer* **2021**, *213*, 123207.
[165] Z. Wang, H. Zuilhof, *Langmuir* **2016**, *32*, 6571.
[166] H. Chen, C. Zhao, M. Zhang, Q. Chen, J. Ma, J. Zheng, *Langmuir* **2016**, *32*, 3315.
[167] F. Koschitzki, R. Wanka, L. Sobota, H. Gardner, K. Z. Hunsucker, G. W. Swain, A. Rosenhahn, *Langmuir* **2021**, *37*, 5591.
[168] P. H. Corkhill, A. M. Jolly, C. O. Ng, B. J. Tighe, *Polymer* **1987**, *28*, 1758.
[169] C. Zhao, J. Zhao, X. Li, J. Wu, S. Chen, Q. Chen, Q. Wang, X. Gong, L. Li, J. Zheng, *Biomaterials* **2013**, *34*, 4714.
[170] C. Zhao, L. Li, J. Zheng, *Langmuir* **2010**, *26*, 17375.
[171] W. Yandi, S. Mieszkin, P. Martin-Tanchereau, M. E. Callow, J. A. Callow, L. Tyson, B. Liedberg, T. Ederth, *ACS Appl. Mater. Interfaces* **2014**, *6*, 11448.
[172] S. Chen, L. Li, C. Zhao, J. Zheng, *Polymer* **2010**, *51*, 5283.
[173] R. Kou, J. Zhang, T. Wang, G. Liu, *Langmuir* **2015**, *31*, 10461.
[174] C. E. Neri-Cruz, F. M. E. Teixeira, J. E. Gautrot, *Chem. Commun.* **2023**, *59*, 7534.
[175] K. Ghosal, S. K. Bhattacharyya, V. Mishra, H. Zuilhof, *Chem. Rev.* **2024**, *124*, 13216.
[176] R. Sivkova, J. Táborská, A. Reparaz, A. de los Santos Pereira, I. Kotelnikov, V. Proks, J. Kučka, J. Svoboda, T. Riedel, O. Pop-Georgievski, *Int. J. Mol. Sci.* **2020**, *21*, 6800.
[177] R. Barbey, E. Kauffmann, M. Ehrat, H.-A. Klok, *Biomacromolecules* **2010**, *11*, 3467.
[178] B. Colak, S. Di Cio, J. E. Gautrot, *Biomacromolecules* **2018**, *19*, 1445.

[179] B. Yang, Y. Wang, M. Vorobii, E. Sauter, M. Koenig, R. Kumar, C. Rodriguez-Emmenegger, M. Hirtz, *Adv. Mater. Interfaces* **2022**, *9*, 2102325.
[180] S. C. Lange, E. van Andel, M. M. J. Smulders, H. Zuilhof, *Langmuir* **2016**, *32*, 10199.
[181] R. Poręba, A. de los Santos Pereira, R. Pola, S. Jiang, O. Pop-Georgievski, Z. Sedláková, H. Schönherr, *Macromol. Biosci.* **2020**, *20*, 1900354.
[182] V. Parrillo, A. de los Santos Pereira, T. Riedel, C. Rodriguez-Emmenegger, *Anal. Chim. Acta* **2017**, *971*, 78.
[183] J. I. Paez, V. Brunetti, M. C. Strumia, T. Becherer, T. Solomun, J. Miguel, C. F. Hermanns, M. Calderón, R. Haag, *J. Mater. Chem.* **2012**, *22*, 19488.
[184] Y. N. Yuksekdag, T. N. Gevrek, A. Sanyal, *ACS Macro Lett.* **2017**, *6*, 415.
[185] H. Lísalová, E. Brynda, M. Houska, I. Víšová, K. Mrkvová, X. C. Song, E. Gedeonová, F. Surman, T. Riedel, O. Pop-Georgievski, J. Homola, *Anal. Chem.* **2017**, *89*, 3524.
[186] H. Vaisocherová-Lísalová, F. Surman, I. Víšová, M. Vala, T. Špringer, M. L. Ermini, H. Šípová, P. Šedivák, M. Houska, T. Riedel, O. Pop-Georgievski, E. Brynda, J. Homola, *Anal. Chem.* **2016**, *88*, 10533.
[187] J. A. Homer, L. Xu, N. Kayambu, Q. Zheng, E. J. Choi, B. M. Kim, K. B. Sharpless, H. Zuilhof, J. Dong, J. E. Moses, *Nat. Rev. Methods Primers* **2023**, *3*, 58.
[188] B. Albada, J. F. Keijzer, H. Zuilhof, F. van Delft, *Chem. Rev.* **2021**, *121*, 7032.
[189] D. Gahtory, R. Sen, A. R. Kuzmyn, J. Escorihuela, H. Zuilhof, *Angew. Chem., Int. Ed.* **2018**, *57*, 10118.
[190] R. Barbey, V. Laporte, S. Alnabulsi, H.-A. Klok, *Macromolecules* **2013**, *46*, 6151.
[191] M. Moazeni, P. Berger, C. Padeste, *Micro Nano Eng.* **2023**, *19*, 100184.
[192] R. M. Hensarling, V. A. Doughty, J. W. Chan, D. L. Patton, *J. Am. Chem. Soc.* **2009**, *131*, 14673.
[193] K. Y. Tan, M. Ramstedt, B. Colak, W. T. S. Huck, J. E. Gautrot, *Polym. Chem.* **2016**, *7*, 979.
[194] P. Costa, J. E. Gautrot, J. T. Connelly, *Acta Biomater.* **2014**, *10*, 2415.
[195] D. P. Nair, M. Podgórski, S. Chatani, T. Gong, W. Xi, C. R. Fenoli, C. N. Bowman, *Chem. Mater.* **2014**, *26*, 724.
[196] S. Tas, M. Kopec´, R. van der Pol, M. Cirelli, I. de Vries, D. A. Bölükbas, K. Tempelman, N. E. Benes, M. A. Hempenius, G. J. Vancso, S. de Beer, *Macromol. Chem. Phys.* **2019**, *220*, 1800537.
[197] S. Neumann, M. Biewend, S. Rana, W. H. Binder, *Macromol. Rapid Commun.* **2020**, *41*, 1900359.
[198] T. N. Gevrek, T. Bilgic, H.-A. Klok, A. Sanyal, *Macromolecules* **2014**, *47*, 7842.
[199] K. Li, J. Chen, Y. Xue, T. Ding, S. Zhu, M. Mao, L. Zhang, Y. Han, *Chem. Eng. J.* **2021**, *423*, 130133.
[200] S. Ravi, V. R. Krishnamurthy, J. M. Caves, C. A. Haller, E. L. Chaikof, *Acta Biomater.* **2012**, *8*, 627.
[201] B. H. Northrop, S. H. Frayne, U. Choudhary, *Polym. Chem.* **2015**, *6*, 3415.
[202] X. M. Sim, C.-G. Wang, X. Liu, A. Goto, *ACS Appl. Mater. Interfaces* **2020**, *12*, 28711.
[203] T. N. Gevrek, A. Degirmenci, R. Sanyal, H.-A. Klok, A. Sanyal, *ACS Appl. Polym. Mater* **2021**, *3*, 2507.
[204] A. R. Kuzmyn, A. T. Nguyen, H. Zuilhof, J. Baggerman, *Adv. Mater. Interfaces* **2019**, *6*, 1900351.
[205] H. Son, J. Ku, Y. Kim, S. Li, K. Char, *Biomacromolecules* **2018**, *19*, 951.
[206] A. T. Nguyen, J. Baggerman, J. M. J. Paulusse, H. Zuilhof, C. J. M. van Rijn, *Langmuir* **2012**, *28*, 604.
[207] M. J. E. Fischer, in *Surface Plasmon Resonance: Methods and Protocols*, (Eds: N. J. Mol, M. J. E. Fischer), Humana Press, Totowa, NJ **2010**.
[208] L. Duque-Sanchez, N. Brack, A. Postma, L. Meagher, P. J. Pigram, *Biomacromolecules* **2019**, *20*, 813.
[209] H. Vaisocherová, V. Ševců, P. Adam, B. Špačková, K. Hegnerová, A. de los Santos Pereira, C. Rodriguez-Emmenegger, T. Riedel, M. Houska, E. Brynda, J. Homola, *Biosens. Bioelectron.* **2014**, *51*, 150.
[210] C. Rodriguez-Emmenegger, O. A. Avramenko, E. Brynda, J. Skvor, A. B. Alles, *Biosens. Bioelectron.* **2011**, *26*, 4545.
[211] A. Hucknall, D.-H. Kim, S. Rangarajan, R. T. Hill, W. M. Reichert, A. Chilkoti, *Adv. Mater.* **2009**, *21*, 1968.
[212] Y. Wang, D. Wang, J. Lin, Z. Lyu, P. Chen, T. Sun, C. Xue, M. Mojtabavi, A. Vedadghavami, Z. Zhang, R. Wang, L. Zhang, C. Park, G. S. Heo, Y. Liu, S. S. Dong, K. Zhang, *Angew. Chem., Int. Ed.* **2022**, *61*, 202204576.
[213] M. Nandimandalam, F. Costantini, N. Lovecchio, L. Iannascoli, A. Nascetti, G. de Cesare, D. Caputo, C. Manetti, *Materials* **2021**, *14*, 7210
[214] N. G. Welch, J. A. Scoble, B. W. Muir, P. J. Pigram, *Biointerphases* **2017**, *12*, 02D301.
[215] D. Kotlarek, M. Vorobii, W. Ogieglo, W. Knoll, C. Rodriguez-Emmenegger, J. Dostálek, *ACS Sens.* **2019**, *4*, 2109.
[216] M. Forinová, A. Seidlová, A. Pilipenco, N. S. Lynn Jr, R. Obořilová, Z. Farka, P. Skládal, A. Saláková, M. Spasovová, M. Houska, L. Kalhotka, H. Vaisocherová-Lísalová, *Curr. Res. Biotechnol.* **2023**, *6*, 100166.
[217] T. Riedel, S. Hageneder, F. Surman, O. Pop-Georgievski, C. Noehammer, M. Hofner, E. Brynda, C. Rodriguez-Emmenegger, J. Dostálek, *Anal. Chem.* **2017**, *89*, 2972.
[218] P. Zhang, F. Sun, H.-C. Hung, P. Jain, K. J. Leger, S. Jiang, *Anal. Chem.* **2017**, *89*, 8217.
[219] J. Wang, Y. Wang, H. Chen, H. Xu, W. Wang, L. Bai, *Sens. Actuators, B* **2018**, *258*, 998.
[220] H. S. Kim, Y. J. Son, W. Mao, K. W. Leong, H. S. Yoo, *Nano Lett.* **2018**, *18*, 314.
[221] M. P. McGowan, A. J. Trowbridge, J. Reitemeier, K. M. Jordan, K. X. Fu, *Biosens. Bioelectron.* **2025**, *276*, 117229.
[222] V. A. Nikitina, A. V. Rudnev, R. R. Nazmutdinov, G. A. Tsirlina, T. Wandlowski, *J. Electroanal. Chem.* **2018**, *819*, 58.
[223] D. Y. Joh, A. M. Hucknall, Q. Wei, K. A. Mason, M. L. Lund, C. M. Fontes, R. T. Hill, R. Blair, Z. Zimmers, R. K. Achar, D. Tseng, R. Gordan, M. Freemark, A. Ozcan, A. Chilkoti, *Proc. Natl. Acad. Sci. USA* **2017**, *114*, E7054.
[224] F. M. Albarghouthi, D. Semeniak, I. Khanani, J. L. Doherty, B. N. Smith, M. Salfity, Q. MacFarlane, A. Karappur, S. G. Noyce, N. X. Williams, D. Y. Joh, J. B. Andrews, A. Chilkoti, A. D. Franklin, *ACS Nano* **2024**, *18*, 5698.
[225] K. B. Buhl, A. H. Agergaard, M. Lillethorup, J. P. Nikolajsen, S. U. Pedersen, K. Daasbjerg, *Polymers* **2020**, *12*, 1475.
[226] A. R. Kuzmyn, S. de Beer, *Polymer* **2025**, *323*, 128155.
[227] T. Zhang, Y. Du, J. Kalbacova, R. Schubel, R. D. Rodriguez, T. Chen, D. R. T. Zahn, R. Jordan, *Polym. Chem.* **2015**, *6*, 8176.
[228] T. Zhang, Y. Du, F. Müller, I. Amin, R. Jordan, *Polym. Chem.* **2015**, *6*, 2726.
[229] M. Flejszar, K. Ślusarczyk, P. Chmielarz, J. Smenda, K. Wolski, M. Wytrwal-Sarna, M. Oszajca, *Polymer* **2022**, *257*, 125268.
[230] S. Lyu, D. Untereker, *Int. J. Mol. Sci.* **2009**, *10*, 4033.
[231] S. Ardalan, A. Ignaszak, *Adv. Sens. Res.* **2024**, *3*, 2300132.
[232] Y. Wang, J. Feng, Z. Tan, H. Wang, *Biosens. Bioelectron.* **2014**, *60*, 218.
[233] J. Veselinovic, S. Almashtoub, E. Seker, *Anal. Chem.* **2019**, *91*, 11923.

[234] J. Y. Yun, K. Y. Kim, Y. J. Park, presented at 2018 IEEE International Conference on Electron Devices and Solid State Circuits (EDSSC), **2018**, pp. 6–8.
[235] S. Saxena, P. Sen, L. Soleymani, T. Hoare, *Adv. Sens. Res.* **2024**, *3*, 2300170.
[236] C. Y. Lim, N. A. Owens, R. D. Wampler, Y. Ying, J. H. Granger, M. D. Porter, M. Takahashi, K. Shimazu, *Langmuir* **2014**, *30*, 12868.
[237] C. M. Fontes, R. K. Achar, D. Y. Joh, I. Ozer, S. Bhattacharjee, A. Hucknall, A. Chilkoti, *Langmuir* **2019**, *35*, 1379.
[238] R. K. Bose, K. K. S. Lau, *Chem. Vap. Deposition* **2009**, *15*, 150.
[239] E. Sevgili, M. Karaman, *Thin Solid Films* **2019**, *687*, 137446.
[240] A. Asatekin, M. C. Barr, S. H. Baxamusa, K. K. S. Lau, W. Tenhaeff, J. Xu, K. K. Gleason, *Mater. Today* **2010**, *13*, 26.
[241] K. Chan, K. K. Gleason, *Langmuir* **2005**, *21*, 8930.
[242] K. Unger, R. Resel, A. M. Coclite, *Macromol. Chem. Phys.* **2016**, *217*, 2372.
[243] K. Chan, L. E. Kostun, W. E. Tenhaeff, K. K. Gleason, *Polymer* **2006**, *47*, 6941.
[244] M. Sun, H. Qiu, C. Su, X. Shi, Z. Wang, Y. Ye, Y. Zhu, *ACS Appl. Bio Mater.* **2019**, *2*, 3983.
[245] M. N. Subramaniam, P. S. Goh, E. Sevgili, M. Karaman, W. J. Lau, A. F. Ismail, *Eur. Polym. J.* **2020**, *122*, 109360.
[246] C. Chu, S. Liu, H. Xiong, Z. Xiang, Y. Hu, S. Chen, *Langmuir* **2024**.
[247] T. Wu, K. Efimenko, J. Genzer, *J. Am. Chem. Soc.* **2002**, *124*, 9394.
[248] M. Kobayashi, M. Terada, Y. Terayama, M. Kikuchi, A. Takahara, *Macromolecules* **2010**, *43*, 8409.
[249] X. Jia, G. Zhang, W. Li, W. Sheng, C. Li, *J. Polym. Sci., Part A: Polym. Chem.* **2014**, *52*, 1807.
[250] R. R. Patil, S. Turgman-Cohen, J. Šrogl, D. Kiserow, J. Genzer, *Langmuir* **2015**, *31*, 2372.

Erik J. Postma is working on his Ph.D. at the University of Twente. His research focusses on protein adsorption in electric fields. He started his career at the Hogeschool Utrecht where he obtained his Bachelor of Applied Sciences in organic chemistry. After working in the bioplastic industry, he completed an M.Sc. in molecular life sciences in Wageningen, where he researched more diverse scientific fields. He researched polymer dynamics in nanoparticle composites with laser speckle imaging during his thesis. Nowadays, he works in the ReCoVR consortium on systems that recycle molecules from feed streams with electric fields.

Luc Scheres received his M.Sc. degree in Chemistry and Physics at Utrecht University in 2005. Subsequently, he moved to Wageningen University and obtained his Ph.D. in surface chemistry in 2010 (with highest honors). After postdoctoral work at Eindhoven University, he founded Surfix in 2011 and was leading the company for almost 10 years. Initially, Surfix was a contract research organization in surface chemistry and nanocoatings. In 2021 Surfix pivoted into the development of a point-of-care diagnostics platform and Luc became the CTO of Surfix.

Sissi de Beer obtained her Ph.D. degree at the University of Twente. After postdoctoral fellowships at the Forschungszentrum in Jülich and the University of Toronto, she is now an associate professor at the University of Twente. In her research, Sissi combines molecular modeling with laboratory experiments to design functional polymer surfaces for application in lubrication, sensing, and molecular separations. Since April 2022, Sissi is also the program director of Applied Physics.

Andriy R. Kuzmyn completed the UNESCO/IUPAC Postgraduate Course in Polymer Science at the Czech Academy of Sciences, focusing on polymer biomaterials. He earned his Ph.D. at Wageningen University (2017–2020), developing antifouling surfaces using innovative polymerization techniques. As a Postdoctoral Researcher at Wageningen, he worked on SI-PET-RAFT polymerization and cell-adhesive surfaces. In 2023, he joined the University of Twente, working on scent-sensing using polymer brushes in the NWO OBSeRVeD project.

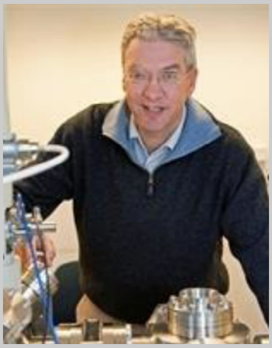

Han Zuilhof is the Chair of Organic Chemistry at Wageningen University. His interests focus on surface organic chemistry and bionanotechnology. He obtained both an M.Sc. in Chemistry (organic chemistry) and an MA in Philosophy (logic and theory of knowledge); both with highest honors. After obtaining a Ph.D. in Chemistry (Leiden University, 1994; highest honors), he did postdoctoral work at the University of Rochester, NY and Columbia University. Subsequently, he joined the faculty at Wageningen University in 1997, moved through the ranks, and has been a Professor of Organic Chemistry since 2007.